博士論文

Impaired development and dysfunction of endothelial progenitor cells in type 2 diabetic mice, assessed using a new mouse endothelial progenitor cell colony-forming assay

（新規マウス血管内皮前駆細胞コロニーフォーミングアッセイを用いた
2 型糖尿病マウスにおける血管内皮前駆細胞の分化能及び機能解析）

塚田　信津

Table of contents

Abbreviations

acLDL	: acetylated-low density lipoprotein
acLDL-DiI	: 1,1'-dioctadecyl-3,3,3',3-tetramethyl-indocarbocyanine perchlorate-labeled acetylated-low density lipoprotein
BM	: bone marrow
BM-KSL	: bone marrow c-Kit+/Sca-1+ lineage-negative cell
BM-LNneg	: lineage-negative bone marrow cell
BM-MNC	: bone marrow mononuclear cell
bp	: base pairs
BrdU	: bromodeoxyuridine
CFU	: colony-forming unit
CFU-EC	: colony-forming unit-endothelial cell
EC	: endothelial cell
ECFC	: endothelial colony-forming cell
EDTA	: ethylenediaminetetraacetic acid
eNOS	: endothelial nitric oxide synthase
EPC	: endothelial progenitor cell
EPC-CFA	: endothelial progenitor cell colony-forming assay
EPC-CFU	: endothelial progenitor cell colony-forming unit
FBS	: fetal bovine serum
FCM	: flow cytometry
FITC	: fluorescein isothiocyanate
GM	: granulocyte macrophage
HIF-1	: hypoxia-inducible factor-1
large-EPC-1	: large-endothelial progenitor cell derived from small-endothelial progenitor cell
PB-MNC	: peripheral blood mononuclear cell
PBS	: phosphate-buffered saline
PCR	: polymerase chain reaction
RT-PCR	: reverse transcription-polymerase chain reaction
SDF-1	: stromal-cell-derived factor-1
T2D	: type 2 diabetes
VE	: vascular endothelial

1. Introduction

1.1 Endothelial progenitor cells development and the 'evaluation system' for endothelial progenitor cells in various ischemic diseases

Endothelial progenitor cells (EPCs) were found in adult peripheral blood in 1997 and were shown to originate from bone marrow [1-3]. EPCs can enter circulation, migrate into ischemic tissue, contribute to postnatal physiologic and pathological neovascularization and play an important role in the restoration of ischemic vascular diseases (Figure 1) [2-5].

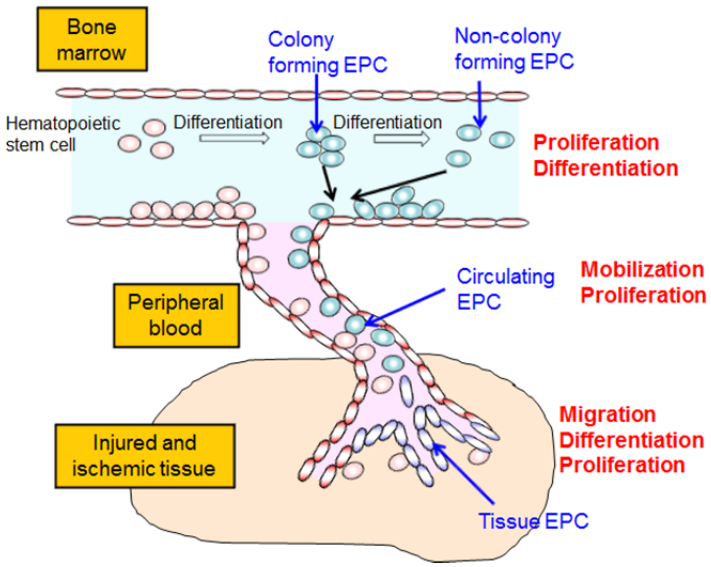

Figure 1 EPC kinetics.

EPCs originate from bone marrow. EPCs can enter circulation, migrate into ischemic tissue and contribute to postnatal physiologic and pathological neovascularization.

Recently, several independent groups have shown that transplantation of EPCs into ischemic hindlimb or myocardial tissue improves organ function following the growth of new vessels [6-11]. In clinical aspects, the frequency of circulating EPCs may also serve as a biomarker for vascular function, and the number of circulating EPCs has been reported to be reduced in patients with diabetes mellitus or risk factors for coronary artery disease and to negatively correlate with the Framingham cardiovascular risk score [12-15]. However, the actual mechanical status of EPC development and the 'evaluation system' for EPC dysfunctions in patients with various ischemic diseases remain to be disclosed.

Because EPCs accumulate in ischemic injured tissues and repair injured tissue following cluster formation [1,2,9], not only the number of EPCs identified by uptake of acetylated-low density

lipoprotein (acLDL) and lectin reactivity but also the colony-forming potential of EPCs is important for angiogenic therapy. Thus, the assay system in which colony-forming potential of EPCs can be assessed is important. EPCs should encompass a group of cells existing in a variety of stages, ranging from hemangioblastic hematopoietic stem cells to fully differentiated endothelial cells (ECs), and EPCs can be classified into stages according to differentiation levels in each circulating EPC and tissue EPC (Figure 1) [16]. Recently, the methods to culture colony-forming unit-endothelial cells (CFU-ECs) [14] or to culture endothelial colony-forming cells (ECFCs) were established on mononuclear cells from peripheral blood or cord blood [17-20]. However, it was reported that CFU-ECs were not EPCs but were myeloid cells that differentiate into phagocytic macrophages and that T cells could mimic the morphology of CFU-ECs [19,21]. Besides, the culture of ECFCs enables us to evaluate the EPC colony-forming potential change as EPCs differentiated during culture *in vitro*. In these assay systems, each EPC at different differentiation levels could not be discriminated at the same time, and the differentiation capacities of immature stem cells could not be tested. Recently, endothelial progenitor cell colony-forming assay (EPC-CFA), a novel method to assess the colony-forming potential of EPCs at different differentiation levels, was established and enables us to investigate the commitment of each cell [22-25].

The aim of the present study is to methodologically establish the murine EPC-CFA on peripheral blood mononuclear cells (PB-MNCs), bone marrow mononuclear cells (BM-MNCs), or bone marrow c-Kit+/Sca-1+ lineage-negative cells (BM-KSL) by analyzing the functions of each EPC-CFU at different differentiation levels and to clarify the roles of each endothelial progenitor cell colony-forming unit (EPC-CFU) at different differentiation levels *in vivo* by using hindlimb ischemic mice. By EPC-CFA, the status of EPC differentiation in response to ischemic signals and the effects of two types of EPC-CFUs, small-EPC-CFUs or large-EPC-CFUs, were investigated in a hindlimb ischemia model on *in vivo* neovascularization.

1.2 Endothelial progenitor cells in type 2 diabetes

EPC dysfunction is involved in a variety of vascular diseases [2,4,5,7,9,10]. Recently, various studies have shown that EPC dysfunction in patients at risk of cardiovascular disease contributes to the development of atherosclerosis and ischemic vascular diseases [14,26]. In particular, patients with type 2 diabetes (T2D) are at increased risk of atherosclerotic disease and poor outcomes after vascular occlusion, and also have a large number of associated complications, such as microvascular diseases [27-29]. Several studies have shown a negative correlation between the number of EPCs and HbA_{1c} levels in T2D patients, as well as the role of EPC dysfunction in adhesion, proliferation and tubular formation in diabetes [12,13]. However, while the colony-forming capacity of EPCs and underlying mechanisms of EPC dysfunction are as yet not

fully understood, their elucidation could aid the development of EPC-recovery-based therapies for microvascular and other ischemic diseases in T2D patients, as the colony-forming potential of EPCs is important for angiogenic therapy. Moreover, increase of inflammation is shown to cause the diabetes complications (Figure 2).

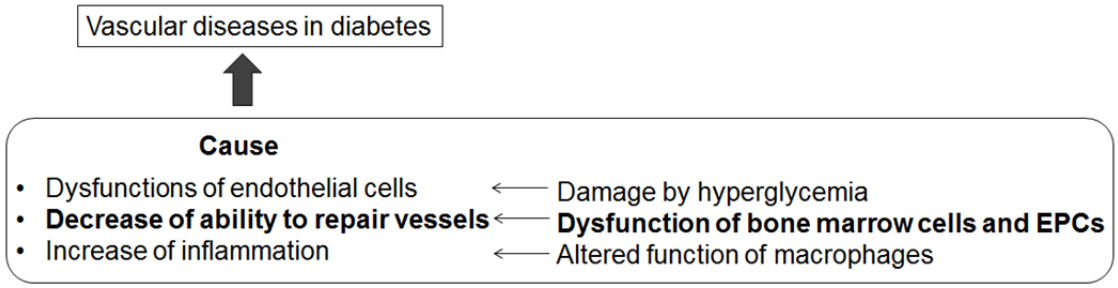

Figure 2 Causes involved in vascular diseases in diabetes.

Thus, the present study aimed to examine the colony-forming capacity of EPCs and differentiation potential of BM-KSL in T2D mice, *db/db* mice and *KKAy* mice, using EPC-CFA. As BM-KSL have the plasticity to transdifferentiate into various cell types and given the close link established between the pathogenesis of T2D and inflammation, this study concomitantly investigated both the differentiation of BM-KSL into hematopoietic cells and development of vascular lineage cells in T2D mice.

1.3 Report structure

The aim of this study is 1) to methodologically establish the murine EPC-CFA by analyzing the functions of each EPC-CFU at different differentiation levels, 2) to clarify the roles of each EPC-CFU at different differentiation levels *in vivo* by using hindlimb ischemic mice, and 3) to elucidate the development and mechanical dysfunction of EPCs in T2D.

In chapter 2, a murine EPC-CFA has been methodologically established. The abilities of murine EPCs in differentiation, adhesive capacity, proliferative potency, and transplantation *in vitro* and *in vivo* were then examined. In conclusions, it was demonstrated that the EPC-CFA could be a useful way to investigate the differentiation levels of murine EPCs, further providing a crucial clue that large-EPC-CFU status may be more functional or effective EPCs to promote neovascularization.

In chapter 3, in order to elucidate the development and mechanical dysfunction of EPCs in T2D, the colony-forming capacity of EPCs and differentiation potential of BM-KSL were examined in T2D mice, *db/db* mice and *KKAy* mice, using EPC-CFA. In conclusions, T2D affected EPC colony formation and differentiation of stem cells to mature EPCs or haematopoietic cells, suggesting opposing regulatory mechanisms for differentiation into mature EPCs and granulocyte

macrophages (GMs) in T2D mice.

The results and new findings obtained in this study are described below.

2. Identification of mouse colony-forming endothelial progenitor cells for postnatal neovascularization: a novel insight highlighted by new mouse colony-forming assay

2.1 Purpose

In this chapter, the aim of this study is to methodologically establish the murine EPC-CFA on PB-MNCs, BM-MNCs, or BM-KSL by analyzing the functions of each EPC-CFU at different differentiation levels and to clarify the roles of each EPC-CFU at different differentiation levels *in vivo* by using hindlimb ischemic mice. An EPC-CFA in murine EPCs has been established. The abilities of murine EPCs in differentiation, adhesive capacity, proliferative potency, and transplantation *in vitro* and *in vivo* were then examined.

The results and new insights on identification of mouse colony-forming EPCs for postnatal neovascularization in the novel EPC-CFA are described below.

2.2 Materials and methods

2.2.1 Animals

Experiments were performed on male 8- to 10-week-old C57BL/6J mice and BALB/CA-nu/nu mice (Japan Clea, Tokyo, Japan) maintained under a 12-hour light/dark cycle and in accordance with the regulations of Tokai University. Standard laboratory chow and water were available ad libitum. The protocols were approved by guidelines of the Institutional Animal Care and Use Committee of the Isehara Campus, Tokai University School of Medicine, based on the Guide for the Care and Use of Laboratory Animals (National Research Council) (Institutional Review Board ID number 083005).

2.2.2 Preparation

Peripheral blood was obtained from the heart immediately before sacrifice and was separated by Histopaque-1083 (Sigma-Aldrich, St. Louis, MO, USA) density gradient centrifugation (Figure 3), as previously described [30]. Briefly, low-density mononuclear cells were harvested and washed twice with Dulbecco's phosphate-buffered saline (PBS) supplemented with 2 mmol/L ethylenediaminetetraacetic acid (EDTA). Contaminated red blood cells were hemolyzed by using ammonium chloride solution. BM-MNCs were obtained by flushing the femurs and tibias and reacted with a mixture of biotinylated monoclonal antibodies against B220 (RA3-6B2), CD3 (145-2C11), CD11b (M1/70), TER-119 (Ly-76), and Gr-1 (RB6-8C5) (all from BD Pharmingen, San Diego, CA, USA) as lineage markers to deplete lineage-positive cells from BM-MNCs by using AutoMACS (Becton Dickinson, Franklin Lakes, NJ, USA) (Figure 3). Lineage-negative bone marrow cells (BM-LNneg) were incubated with saturating concentrations of directly labeled anti-c-Kit (at 1:25 dilution) (BD Biosciences, Franklin Lakes, NJ, USA) and anti-Sca-1 antibodies

(at 1:25 dilution) (BD Biosciences) for 30 minutes on ice, and then the c-Kit+/Sca-1+ lineage-negative cells (BM-KSL) were isolated with live sterile cell sorting (FACSVantage SE; Becton Dickinson) (Figure 3).

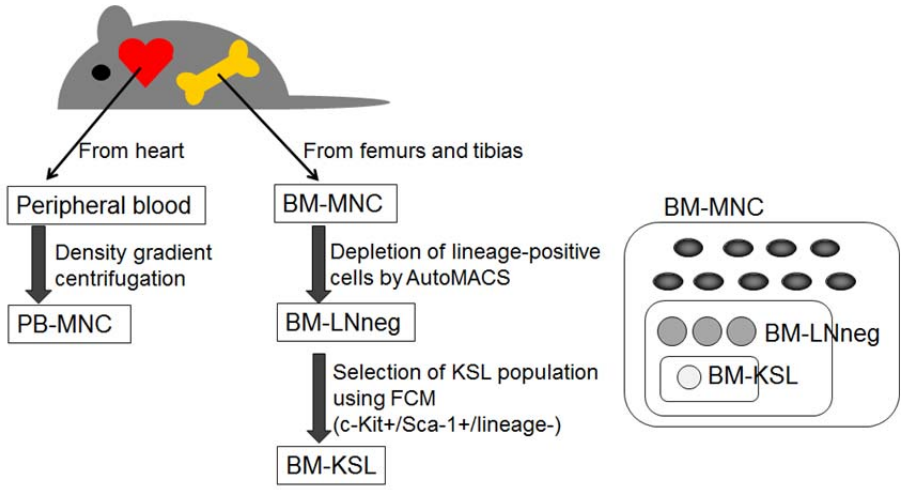

Figure 3 Schematic of preparation protocol.

2.2.3 Endothelial progenitor cell colony-forming assay

Various cells were cultured in methylcellulose-containing medium M3236 (StemCell Technologies, Vancouver, BC, Canada) with 20 ng/mL stem cell-derived factor (Kirin, Tokyo, Japan), 50 ng/mL vascular endothelial (VE) growth factor (R&D Systems, Minneapolis, MN, USA), 20 ng/mL interleukin-3 (Kirin), 50 ng/mL basic fibroblast growth factor (Wako, Osaka, Japan), 50 ng/mL epidermal growth factor receptor (Wako), 50 ng/mL insulin-like growth factor-1 (Wako), 2 U/mL heparin (Ajinomoto, Tokyo, Japan), and 10% fetal bovine serum (FBS) on a 35-mm dish for 8 days. Cell densities for each sample were as follows: PB-MNCs 7×10^5 cells per dish, BM-MNCs 1×10^4 cells per dish, BM-LNneg 2.5×10^3 cells per dish, and BM-KSL 500 cells per dish. The EPC-CFUs were identified as large-EPC-CFUs or small-EPC-CFUs by visual inspection with an inverted microscope under 40× magnification. Large-EPC-CFUs were composed of spindle-shaped cells, and small-EPC-CFUs were composed of round adhesive cells.

2.2.4 Endothelial progenitor cell colony-forming unit staining

After 8 days in culture, the EPC-CFU cultures were treated with 0.4 μg/mL 1,1'-dioctadecyl-3,3,3',3-tetramethyl-indocarbocyanine perchlorate-labeled acLDL (acLDL-DiI; Biomedical Technologies Inc., Stoughton, MA, USA) for 1 hour and fixed by application of 1 mL of 2% paraformaldehyde for 1 hour at room temperature. After a wash of the methylcellulose-containing medium with PBS, the cultures were reacted with fluorescein

isothiocyanate (FITC)-conjugated BS-1 lectin (Sigma-Aldrich) for 1 hour at room temperature. After a wash with PBS, the cultures were observed under a fluorescence microscope (IX70; Olympus, Tokyo, Japan).

2.2.5 Large-endothelial progenitor cell or small-endothelial progenitor cell isolation

Cells composed of small-EPC-CFUs were collected with a pipette under a microscope as small-EPCs. Then the cultures were washed with PBS, and large-EPCs were harvested after treatment with 2 mmol/L EDTA/PBS. For the purpose of cell transplantation into a hindlimb ischemia model, non-attached cells were isolated as small-EPCs by washing with PBS, whereas attached cells were harvested as large-EPCs by treatment with EDTA/PBS (5 mmol/L) for 5 minutes at 37°C.

2.2.6 Adhesive assay

Culture plates (24-well) were coated with human fibronectin (100 μg/mL; Gibco, now part of Invitrogen Corporation, Carlsbad, CA, USA). Large-EPCs or small-EPCs (2×10^4 cells per well) were allowed to attach in EGM-2 (Cambrex Bio Science Walkersville, Walkersville, MD, USA) for 20 minutes at 37°C, and the non-adherent cells were aspirated. The adherent population was fixed with 1% paraformaldehyde for 20 minutes and stored in PBS. The numbers of adherent cells were quantified from counts in six random microscopic fields per well.

2.2.7 Proliferation assay

At day 7, EPC-CFU cultures were treated with 10 μmol/L bromodeoxyuridine (BrdU) (Sigma-Aldrich) and incubated for 24 hours. BrdU positivities of large-EPCs or small-EPCs were analyzed by using BrdU flow kits (BD Pharmingen) and a fluorescence-activated cell sorter, as previously described [31].

2.2.8 Tubular formation assay

Two-week derived CD133(-) mononuclear cells of human cord blood were used as ECs. These cells were confirmed to be ECs by tubular formation and immunocytochemistry of endothelial nitric oxide synthase (eNOS), kinase insert domain receptor (KDR), and VE-cadherin (data not shown) [5]. Each small-EPC or large-EPC was labeled with acLDL-DiI for 1 hour. After washing of the labeled small-EPCs or large-EPCs with PBS, the 1×10^3 cells were mixed together with 1.2×10^4 ECs in 50 μL of 2% FBS/EBM-2. Cell suspension (50 μL) was applied onto 50 μL of Matrigel (BD, Franklin Lakes, NJ, USA) per well of a 96-well plate (BD Falcon, Franklin Lakes, NJ, USA) and then incubated for 8 hours. After incubation, the numbers of tubular formation were counted on a display of Photoshop software (Adobe, San Jose, CA, USA) after a picture per well was taken at

40× magnification under a light microscope (Eclipse TE300; Nikon, Tokyo, Japan). The numbers of incorporated labeled cells into tubes were also counted on a display of Photoshop software after a picture per well was taken at 100× magnification under a fluorescence microscope.

2.2.9 Secondary culture

Isolated small-EPCs (5×10^4) were suspended in 50 μL of Iscove's modified Dulbecco's medium (Gibco) and applied onto 100 μL of methylcellulose-containing medium per well of a 96-well plate (BD Falcon). After 2 days of incubation, methylcellulose-containing medium was changed to Iscove's modified Dulbecco's medium containing acLDL-DiI and BS-1 lectin-conjugated FITC and then incubated for 1 hour. After a wash with PBS, cultures were observed under a fluorescence microscope.

2.2.10 Reverse transcription-polymerase chain reaction

Total RNA of small-EPCs or large-EPCs was prepared with an RNeasy Micro/Mini kit (Qiagen, Valencia, CA, USA). Reverse transcription-polymerase chain reaction (RT-PCR) was performed by using Superscript III Reverse Transcriptase (Invitrogen Corporation) with 1 μg of total RNA. PCR amplification was then performed with synthetic gene-specific primers for eNOS (forward primer, 5'-GGATTGTGTCACTTCGTTCGGT-3'; reverse primer, 5'-CAGCAGGATGCCCTAACTACCA-3'; product length, 183 base pairs (bp)), Flk-1 (forward primer, 5'-AAAGAGAGGAACGTCGGCAGA-3'; reverse primer, 5'-AAGCACACAGGCAGAAACCAGT-3'; product length, 376 bp), VE-cadherin (forward primer, 5'-AGATTCACGAGCAGTTGGTCA-3'; reverse primer, 5'-GATGTCAGAGTCGGAGGAATT-3'; product length, 355 bp), and β-actin (forward primer, 5'-AACACCCCAGCCATGTACGTA-3'; reverse primer, 5'-AAGGAAGGCTGGAAAAGAGCC-3'; product length, 416 bp) by using exTaq polymerase (Takara, Kyoto, Japan). To quantify transcripts, semi-quantitative RT-PCRs were performed and normalized to Actb, which encodes β-actin. PCRs were performed at 94°C for 45 seconds, 64°C for 1 minute, and 72°C for 1 minute for 35 or 33 or 22 cycles and analyzed on 2% agarose gels.

2.2.11 Flow cytometry

For flow cytometry (FCM) analysis, the monoclonal antibodies specific to Sca-1 and c-Kit were used. BM-LNneg or EPC-CFU-derived cells were incubated with directly labeled anti-Sca-1 (at 1:100 dilution) and anti-c-Kit (at 1:100 dilution) antibodies for 30 minutes on ice. The cells were analyzed by two-color flow cytometry by using a FACS caliber (Becton Dickinson).

2.2.12 Animal model of ischemic hindlimb

Unilateral hindlimb ischemia was created in C57BL/6J mice or BALB/CA-nu/nu as previously described [32]. Briefly, the animals were anesthetized with Nembutal (60 mg/kg intraperitoneally; Dainippon Sumitomo Pharma Co., Osaka, Japan) and then an incision in the skin overlying the middle portion of the left hindlimb was performed. After ligation of the proximal end of the femoral artery, the distal portion of the saphenous artery was ligated and the artery, as well as all side branches, was dissected free and excised. The skin was closed by using a surgical stapler.

2.2.13 Monitoring of hindlimb blood flow

After anesthesia, hindlimb perfusion was measured by using a laser Doppler perfusion imaging system (Moor Instruments, Wilmington, DE, USA). The stored perfusion values behind the color-coded pixels representing the microvascular blood flow distribution are available for analysis. Color photographs were recorded and analysis performed by calculating the average perfusion of the ischemic and non-ischemic foot. To account for variables such as ambient light and temperature, the results are expressed as the ratio of perfusion in the left (ischemic) versus right (normal) limb. In the EPC transplantation experiment, isolated small-EPCs, large-EPCs, or murine ECs (2.5×10^5) derived from the aorta of C57BL/6J were transplanted into hindlimb induced nude mice by intramuscular injection, respectively (n = 8).

2.2.14 Measuring of capillary density

Twenty-eight days after ischemia, capillary density was determined in tissue sections from the lower calf muscles of ischemic and healthy limbs by expressed as number of CD31(+) cells as ECs per myocyte. To stain the capillary, a staining procedure was performed with rat anti-mouse CD31 antibodies (BD Biosciences) or Alexa-fluor 594 (Molecular Probes, now part of Invitrogen Corporation) anti-iso-lectin B4 reagents (Sigma-Aldrich).

2.2.15 Statistical analysis

All data were presented as mean ± standard deviation. P values were calculated by using the unpaired Student t test. For the analysis of *in vivo* ischemia experiments, the Scheffe's test was performed for the multiple comparisons after analysis of variance between each group. A P value of less than 0.05 was considered statistically significant.

2.3 Results

2.3.1 Development of murine endothelial progenitor cell colony-forming assay

To address the detail functions and actual status of *in vivo* EPCs, a novel EPC-CFA in murine EPCs was first established (Figure 4A). After culture of PB-MNCs, BM-MNCs, or BM-KSL of

C57BL/6J mice in growth factor-containing methylcellulose medium, these primitive cells differentiated into two types of EPC colony clusters: large-EPC-CFUs and small-EPC-CFUs (Figure 4B, data not shown). Morphologically, these cells are large-EPC-CFUs, which were composed mainly of spindle/round-shaped cells, whereas cells composed of small-EPC-CFUs were round. Both EPC-CFUs differentiated from primary PB-MNCs or primary bone marrow (BM)-derived cells were identified as EPCs by acLDL uptake and BS-1 lectin reactivity, a typical feature of characterization of endothelial lineage cells (Figure 4C-E, data not shown). The frequencies of large-EPC-CFUs or small-EPC-CFUs differentiated from 7×10^5 PB-MNCs were 2.8 ± 1.3 and 6.0 ± 2.0 per dish, respectively. The normalized frequencies of large-EPC-CFUs or small-EPC-CFUs differentiated from 7×10^5 BM-MNCs were 665 ± 309 and 852 ± 82 per dish, respectively (Figure 4F). These results revealed that BM-MNCs had higher EPC colony-forming capacity than PB-MNCs. In this EPC-CFA, EPCs from primary murine cells could be classified into two types of EPC-CFUs and the colony-forming potential could be assessed by the frequency of EPC-CFUs. To check the commitment of each EPC-CFU-derived cell, eNOS, Flk-1, and VE-cadherin, markers of ECs, were examined. Gene expression profiles revealed that large-EPCs and small-EPCs expressed eNOS, Flk-1, and VE-cadherin gene in both PB-MNCs and BM-MNCs (Figure 4G), showing that large-EPCs strongly expressed VE-cadherin, a typical EC marker, although small-EPCs also expressed eNOS or Flk-1, each of which is a committed marker of endothelial lineage cells.

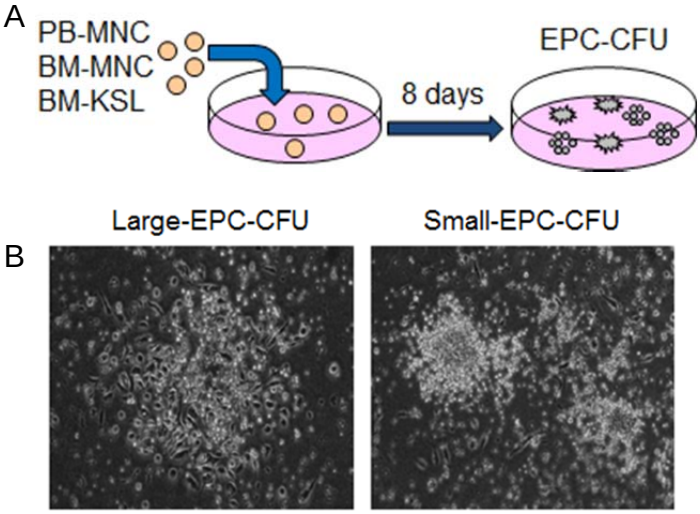

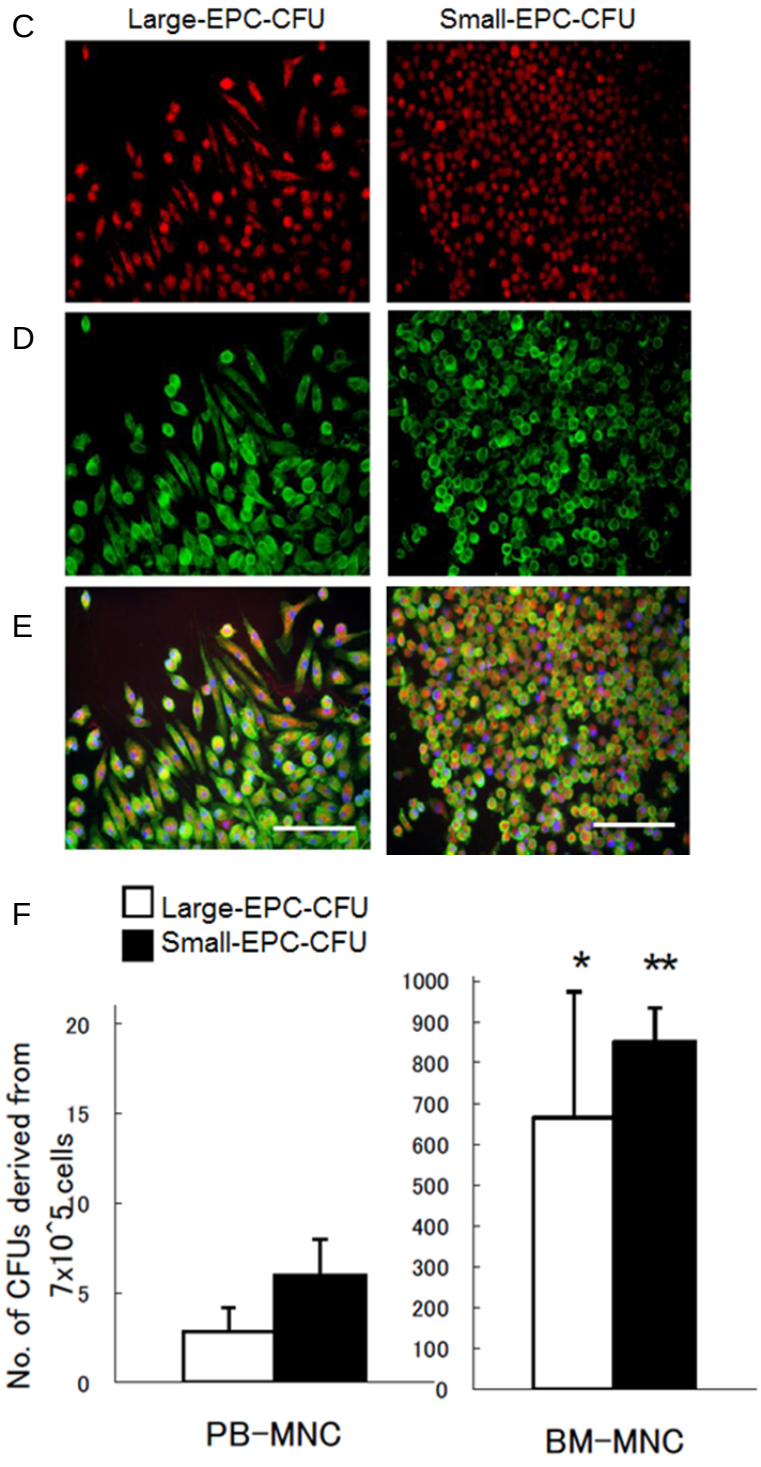
C
Large-EPC-CFU
Small-EPC-CFU
D
E
F
Large-EPC-CFU
Small-EPC-CFU
No. of CFUs derived from 7x10^5 cells
20
15
10
5
0
1000
900
800
700
600
500
400
300
200
100
0
*
**
PB-MNC
BM-MNC

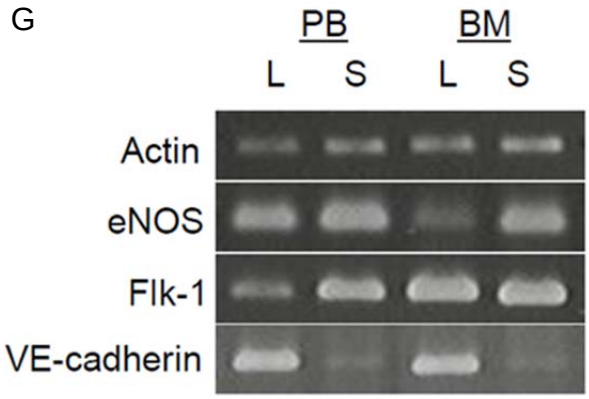

Figure 4 Murine endothelial progenitor cell colony-forming units (EPC-CFUs).

A. Schematic of EPC-CFA protocol. B. Representative micrographs of large-EPC-CFUs or small-EPC-CFUs cultured from BM-MNCs for 8 days. Large-EPC-CFUs and small-EPC-CFUs were defined according to cell morphology as spindle-shaped cells or round cells, respectively. C-E. EPC-CFUs were identified as double-positive cells due to acLDL-DiI uptake (red) and BS-1 lectin reactivity (green). Scale bar represents 100 μm. F. EPC colony-forming assay in murine PB-MNCs or BM-MNCs. The frequencies of large-EPC-CFUs (white columns) or small-EPC-CFUs (black columns) from PB-MNCs or BM-MNCs (7×10^5 cells) were counted after 8 days of culture. *$P < 0.05$, **$P < 0.01$ versus PB-MNC-derived EPC-CFUs. G. Expression patterns of eNOS, Flk-1, and VE-cadherin genes in large-EPCs (L) or small-EPCs (S) from PB-MNCs or BM-MNCs. Both EPC-CFU-derived cells expressed markers of ECs.

2.3.2 Characterization of large-endothelial progenitor cells or small-endothelial progenitor cells

To characterize these two types of EPC-CFUs (large-EPC-CFUs or small-EPC-CFUs), EPC-CFU-derived cells were separately collected and the functions of both EPC-CFUs were investigated. To determine the proliferation potency of each EPC-CFU-derived cell, a proliferation assay was performed. In PB-MNCs-derived EPC-CFUs, 24.5% ± 15.6% of large-EPCs and 51.2% ± 8.8% of small-EPCs incorporated BrdU. In BM-MNCs-derived EPC-CFUs, 17.1% ± 13.9% of large-EPCs and 46.4% ± 23.0% of small-EPCs incorporated BrdU (Figure 5A). More small-EPCs incorporated BrdU than large-EPCs, suggesting that large-EPCs have lower proliferation potency than small-EPCs. From observation of EPC-CFUs under a microscope, small-EPC-CFUs were constituted of more cells than large-EPC-CFUs and the areas of small-EPC-CFUs were significantly larger than those of large-EPC-CFUs (data not shown). Next, an adhesive capacity of these two types of EPC-CFUs was defined. The numbers of adherent large-EPCs or small-EPCs from PB-MNCs were 40.5 ± 7.6 and 26.3 ± 5.6 per field, respectively, and those from BM-MNCs were 63.7 ± 12.0 and 27.2 ± 8.0 per field, respectively (Figure 5B), proving that the large-EPCs

have higher adhesive capacity than small-EPCs by 1.5-fold in PB-MNCs and 2.3-fold in BM-MNCs. To check tube-forming ability, large-EPCs or small-EPCs derived from BM were labeled with acLDL-DiI and cocultured with ECs, which were 2-week derived CD133(-) mononuclear cells of human cord blood, on Matrigel. Fluorescent tagging of each EPC-CFU-derived cell with DiI enabled delineation from ECs (Figure 5C). The number of tubes in coculture with large-EPCs increased significantly compared with small-EPCs (large-EPCs; 78.3 ± 5.8, small-EPCs; 70.7 ± 8.4) (Figure 5D, left). Moreover, more large-EPCs were incorporated into tubes compared with small-EPCs (large-EPCs; 8.3 ± 2.7, small-EPCs; 4.2 ± 1.7) (Figure 5D, right), implying that large-EPCs made a substantial contribution to tubular networks with ECs, although small-EPCs showed minimal incorporation into the developing vascular network. Taken together, three independent results strongly indicated that large-EPCs and small-EPCs had different functions and that large-EPCs might be more mature EPCs with respect to adhesion ability and functional contribution of tubule networks of ECs.

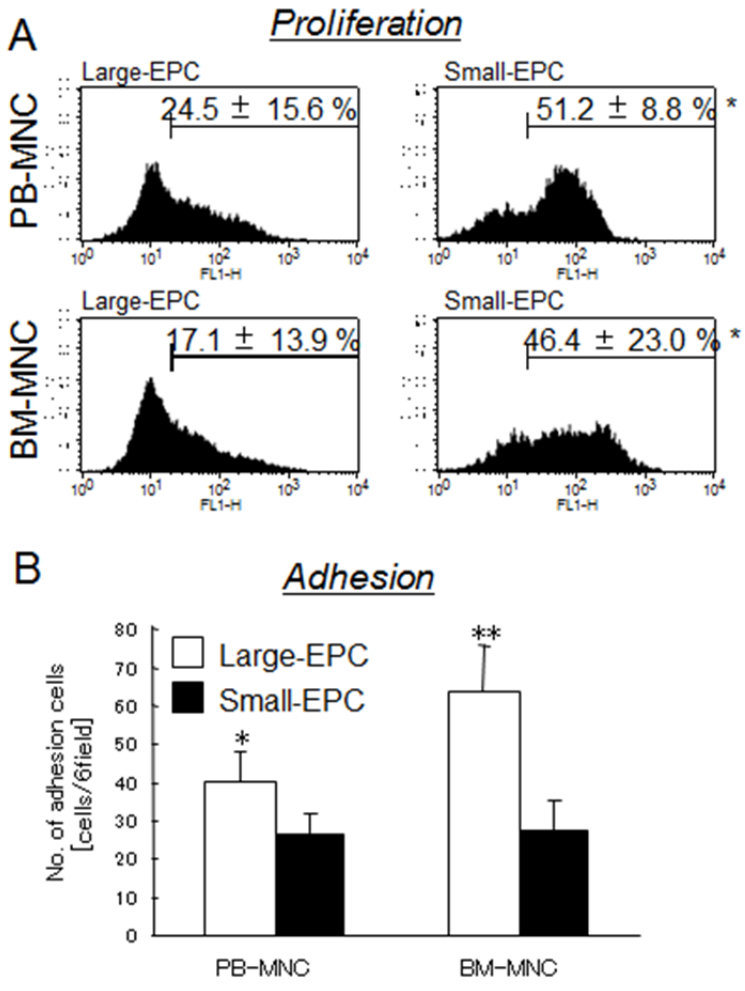

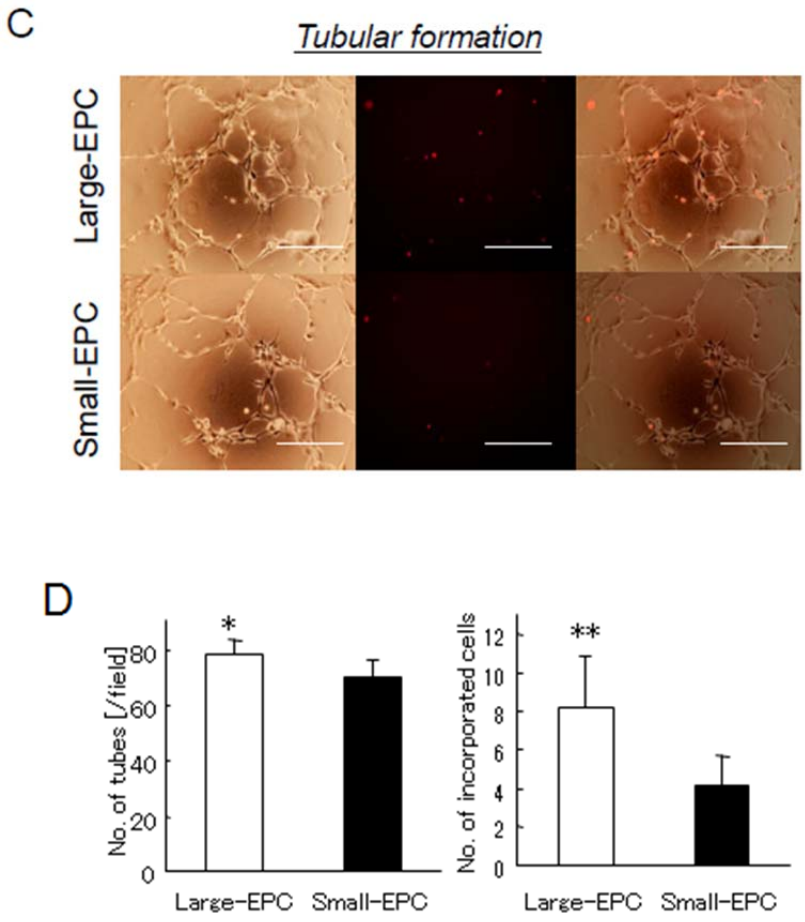

Figure 5　Characterization of large-EPCs or small-EPCs.

A. Proliferation assay of large-EPCs or small-EPCs from PB-MNCs (upper) or BM-MNCs (bottom). After 7 days of culture, large-EPC-CFUs or small-EPC-CFUs were allowed to incorporate BrdU for 24 hours and analyzed by FCM. Large-EPCs had significantly lower proliferative potency than small-EPCs in both PB-MNCs and BM-MNCs (*P < 0.05 versus large-EPCs). B. Adhesion assay of large-EPCs or small-EPCs from PB-MNCs or BM-MNCs. Large-EPCs (white columns) or small-EPCs (black columns) were allowed to adhere to a fibronectin-coated plate for 20 minutes. More large-EPCs had adhesive capacity than small-EPCs. *P < 0.05, **P < 0.01 versus small-EPCs. C. Tubular formation assay of large-EPCs or small-EPCs from BM-MNCs. Large-EPCs or small-EPCs labeled with acLDL-DiI (red) were cocultured with ECs to form tubular structures within Matrigel. Representative light and fluorescent micrographs of ECs cocultured with large-EPCs (upper) and small-EPCs (bottom) are shown. Scale bar represents 500 μm. D. Quantification of the number of tubes (left). Large-EPCs made a substantial contribution to tubular networks with ECs. *P < 0.05 versus small-EPCs. Quantification of the number of cells incorporated into tubes (right). Small-EPCs showed minimal incorporation into the

developing vascular network. **P < 0.01 versus small-EPCs.

2.3.3 Importance of small-endothelial progenitor cells as large-endothelial progenitor cell-colony-forming unit sprouting cells

To determine whether small-EPCs are real immature cells, FCM analysis was performed on EPC-CFU-derived cells, which developed from fresh isolated BM-KSL (c-Kit+/Sca-1+/LNneg, purity of greater than 99.5%) cells. As shown in Figure 6A, the higher population of KSL cells in small-EPCs was observed, providing us a clue that small-EPCs contained actual progenitors. Therefore, to check whether small-EPCs can differentiate into large-EPCs, isolated small-EPCs were reseeded in methylcellulose-containing medium. PB-MNC-, BM-MNC-, or BM-KSL cell-derived-small-EPCs could differentiate into spindle-shaped cells, large-EPCs and could represent positivity of acLDL uptake and BS-1 lectin binding (Figure 6B, data not shown). To characterize small-EPCs-derived large-EPCs, the gene expression of VE-cadherin, Flk-1, and eNOS; adhesion capacity; and incorporation potential of small-EPC-derived large-EPCs (large-EPCs-1) were examined compared with small-EPCs and large-EPCs (large-EPCs-2). Gene expression profiles by RT-PCR revealed that large-EPCs-1 strongly expressed VE-cadherin and Flk-1 compared with small-EPCs (Figure 6C). In the adhesion assay, the numbers of adherent small-EPCs, large-EPCs-1, and large-EPCs-2 were 23.2 ± 5.1, 52 ± 5.3, and 61.5 ± 8.3 per field, respectively (Figure 6D). In the tubular formation assay, more large-EPCs-1 were incorporated into tubes compared with small-EPCs (Figure 6E). These results revealed that the large-EPCs derived from small-EPCs showed a higher potential of VE-cadherin expression, adhesion, and tube formation compared with those of small-EPCs, suggesting that small-EPCs might be more immature EPCs and be early EPCs, which could differentiate into large-EPCs.

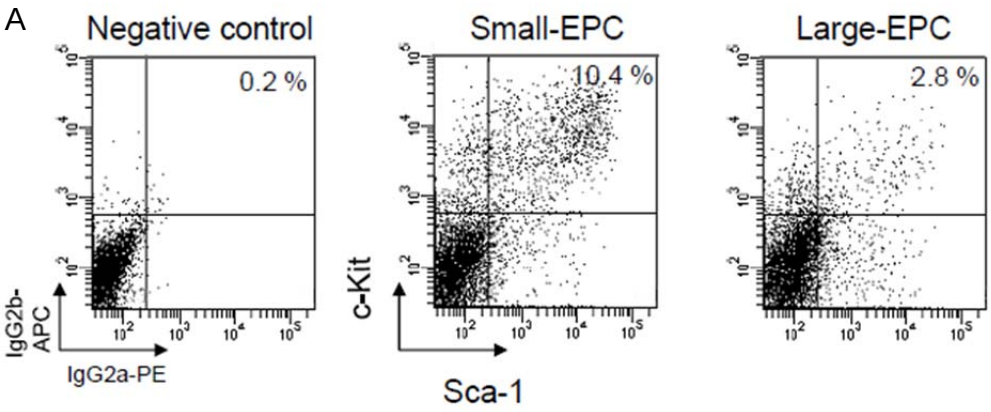

B

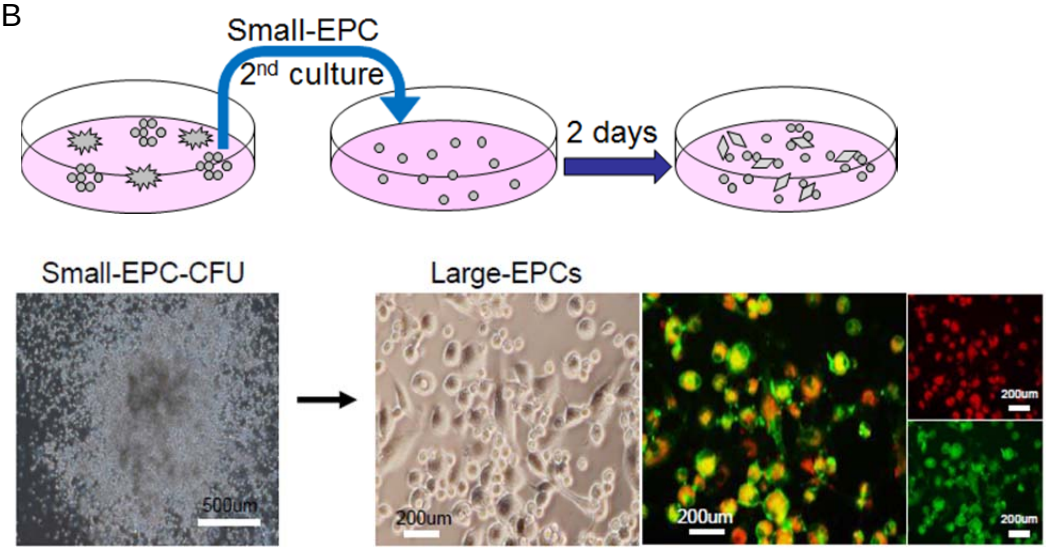
Small-EPC
2nd culture
2 days
Small-EPC-CFU
Large-EPCs
500um
200um
200um
200um
200um

C

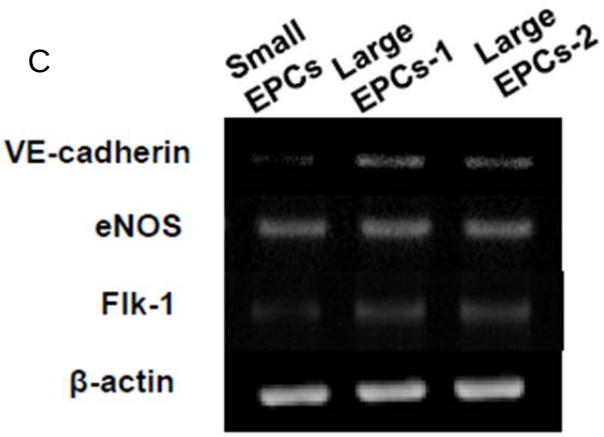
Small EPCs
Large EPCs-1
Large EPCs-2
VE-cadherin
eNOS
Flk-1
β-actin

D

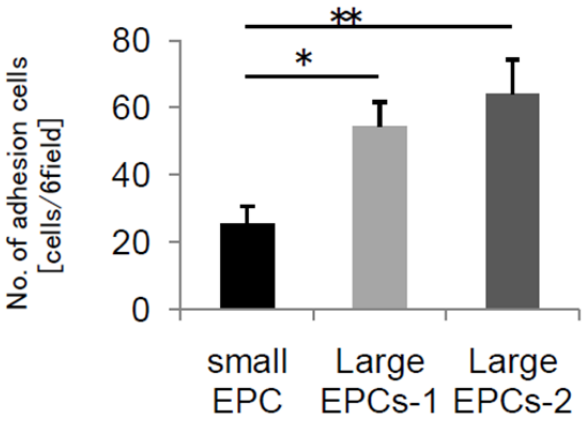
**
*
80
60
40
20
0
No. of adhesion cells [cells/6field]
small EPC
Large EPCs-1
Large EPCs-2

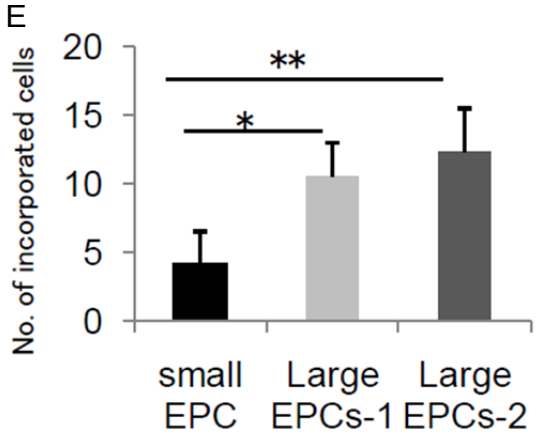

Figure 6 Importance of small-EPCs as large-EPC-CFU-sprouting cells.

A. FCM analysis of small-EPCs or large-EPCs after culturing for 10 days from freshly isolated BM-KSL. B. Secondary culture assay of small-EPC-CFUs from BM-MNCs. Representative micrographs of small-EPC-CFUs from BM-MNCs before reseeding are shown on the left, and representative light and fluorescent micrographs of small-EPCs cultured secondarily in methylcellulose-containing medium are shown on the right. Secondary cultured cells were identified as double-positive cells due to acLDL-DiI uptake (red) and BS-1 lectin reactivity (green). Small-EPCs could differentiate into large-EPCs. C. The expression of VE-cadherin, Flk-1, and eNOS was measured in small-EPCs, small-EPCs-derived large-EPCs (Large-EPCs-1), and large-EPCs (Large-EPCs-2) by RT-PCR analysis. D. Adhesion assay of small-EPCs, Large-EPCs-1, and Large-EPCs-2. *P < 0.05, **P < 0.01 versus small-EPCs. E. Quantification of the number of cells incorporated into tubes in small-EPCs, Large-EPCs-1, and Large-EPCs-2. *P < 0.05, **P < 0.01 versus small-EPCs.

2.3.4 Potentials to produce endothelial progenitor cell colony-forming units of BM-MNCs, BM-LNneg and BM-KSL in endothelial progenitor cell colony-forming assay

To optimize the cell densities of various populations in bone marrow in EPC-CFA, BM-MNCs, BM-LNneg and BM-KSL were respectively cultured at various cell densities. BM-LNneg population was 8.8 % of BM-MNCs and KSL population was 3.8 % of BM-LNneg in C57BL/6J mice. As shown in Figure 7A, the best frequency of EPC-CFUs per dish was from 20 to 30 because it is difficult to count EPC-CFUs in case more than 40 EPC-CFUs could fuse each other in one dish and to detect the changes of the frequencies in case only less than 10 EPC-CFUs appeared in one dish. Thus, the best cell densities of BM-MNCs, BM-LNneg and BM-KSL were $1x10^4$ cells/dish, $2.5x10^3$ cells/dish and 500 cells/dish, respectively. In this EPC-CFA, we calculated the numbers of cells which could produce one EPC-CFU in PB-MNCs, BM-MNCs, BM-LNneg and BM-KSL population. One large-EPC-CFU was derived from $2.1x10^5 \pm 0.8x10^5$ PB-MNCs or $1.1x10^3 \pm$

$0.2x10^3$ BM-MNCs or $3.6x10^2 \pm 1.1x10^2$ BM-LNneg or 57 ± 34 BM-KSL (Figure 7B). And one small-EPC-CFU was derived from $8.2x10^4 \pm 0.2x10^4$ PB-MNCs or $5.5x10^2 \pm 0.7x10^2$ BM-MNCs or $1.2x10^2 \pm 0.2x10^2$ BM-LNneg or 28 ± 3 BM-KSL (Figure 7B). These results demonstrated that BM-MNCs had higher potential to differentiate into EPC-CFUs compared with PB-MNCs and that KSL population produced more EPC-CFUs and might enrich highly immature EPCs in BM.

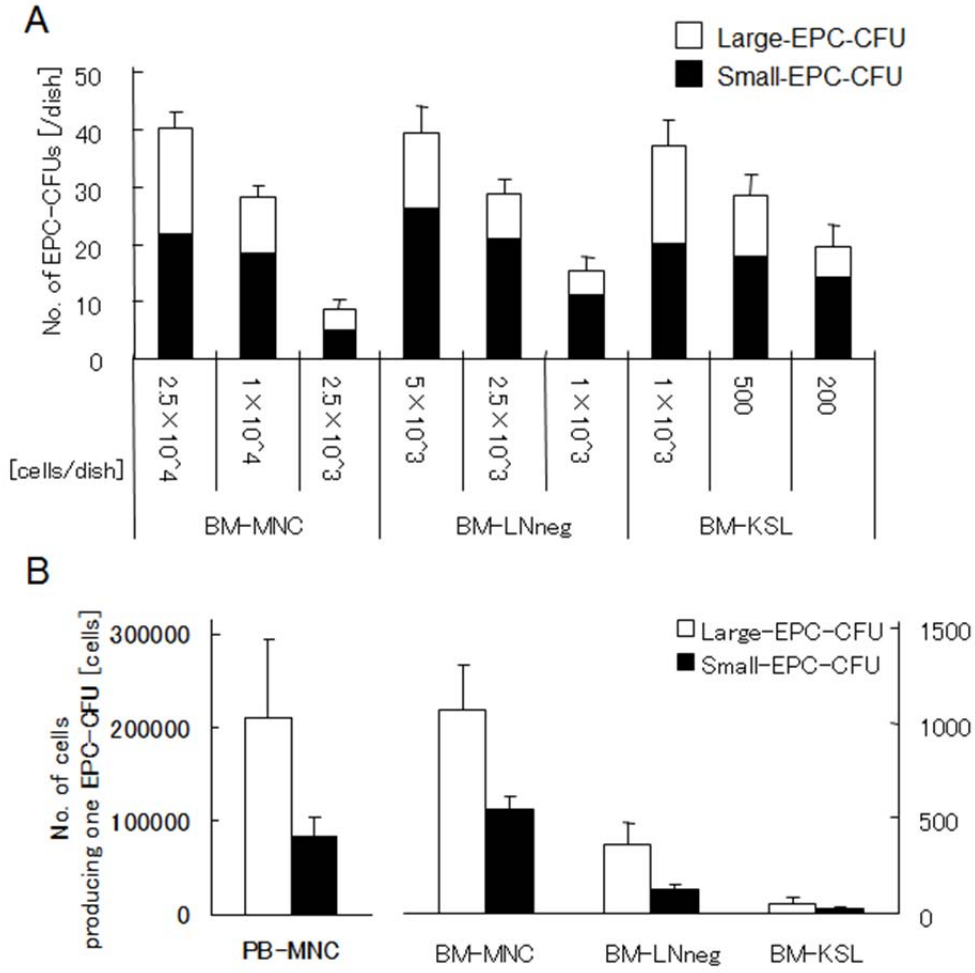

Figure 7　Potentials to produce EPC-CFUs of BM-MNCs, BM-LNneg and BM-KSL in EPC-CFA. A. The frequency of large-EPC-CFUs (white columns) or small-EPC-CFUs (black columns) from various populations of bone marrow at each cell density. B. The number of cells which could produce one EPC-CFU. BM-MNCs had higher potential to differentiate into EPC-CFUs compared with PB-MNCs and KSL population had the highest capacity to differentiate into EPC-CFUs in BM.

2.3.5 Kinetics of endothelial progenitor cell colony-forming units in response to ischemia

EPCs play a critical role in restoration of ischemic diseases. To explore the effects of hindlimb ischemia on differentiation of BM into EPC-CFUs, PB-MNCs and BM of hindlimb ischemic mice were examined in EPC-CFA. This experiment could enable us to elucidate the roles of each EPC-CFU *in vivo*. First, hindlimb perfusion was evaluated by serial laser Doppler perfusion imaging studies at day 5 after surgery. The ratio of blood flow between the ischemic and the normal limb was 0.19 ± 0.16, which was a significant difference compared with 0.98 ± 0.21 in the normal mice (data not shown). To explore the *in vivo* change in BM, the percentage of KSL population in BM was estimated by FCM analysis. The percentage of BM-LNneg did not change, but that of the KSL population in BM-LNneg was 6.6% ± 2.0% in ischemic mice, which was significantly increased compared with the normal mice: 3.8% ± 1.2% (Figure 8A and B). These data demonstrated that BM-KSL cells, which produced more EPC-CFUs, were induced by hindlimb ischemia. To check the differentiation capacities of EPCs from PB-MNCs and various fractions of BM-MNCs, the frequencies of EPC-CFUs from each population were counted. In all populations, the frequencies of large-EPC-CFUs and the ratios of large-EPC-CFUs were significantly increased in hindlimb ischemic mice (Figure 8C). These results indicated that hindlimb ischemia induced the differentiation of PB-MNCs and various populations of BM, implying that large-EPC-CFUs might play an important role in the restoration of ischemic diseases.

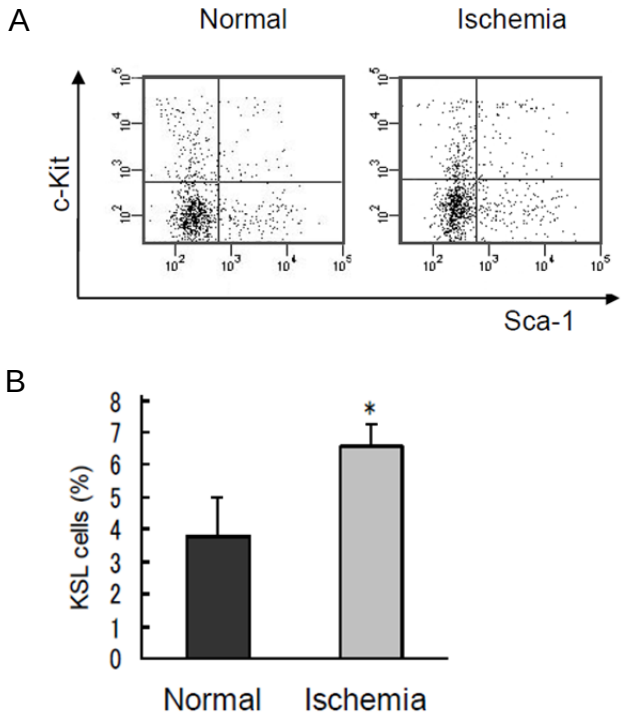

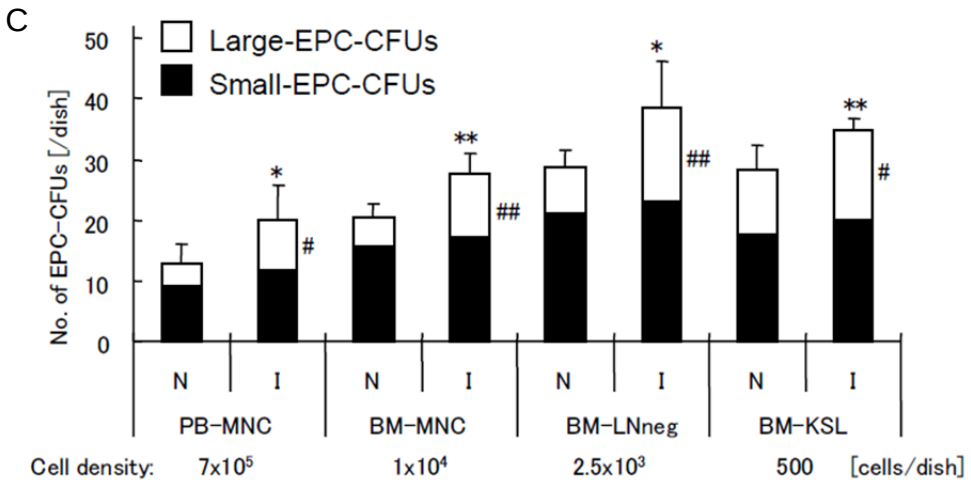

Figure 8 Development of two types of EPC-CFUs in response to ischemia.

A. FCM analysis of BM-LNneg using rat IgG antibodies against mouse c-Kit and Sca-1. B. The percentage of c-Kit+/Sca-1+ population of BM-LNneg. Hindlimb ischemia induced KSL population in bone marrow. *P < 0.05 versus normal mice. C. The frequencies of large-EPC-CFUs (white columns) and small-EPC-CFUs (black columns) from PB-MNCs, BM-MNCs, BM-LNneg, and BM-KSL in normal mice (N) and hindlimb ischemic mice (I). Hindlimb ischemia increased the number of large-EPC-CFUs and total EPC-CFUs differentiated from PB-MNCs and BM. *P < 0.05, **P < 0.01 versus total EPC-CFUs from normal mice. #P < 0.05, ##P < 0.01 versus large-EPC-CFUs from normal mice. Hindlimb ischemia induced the differentiation of PB-MNCs and BM.

2.3.6 Contribution of large-endothelial progenitor cells or small-endothelial progenitor cells to postnatal/adult neovascularization

To determine the functional importance of *in vivo* EPC status in a pathological situation, large-EPCs or small-EPCs and murine ECs as controls were transplanted into hindlimb ischemia models. As shown in Figure 9A and B, the limb salvage was observed in large-EPC transplantation groups, although small-EPC, EC, or PBS transplantation groups did not operate as useful limb therapy cells. These macroscopical observations were further supported by monitoring of real blood flow by using a laser Doppler perfusion imaging system because the recovery of limb perfusion was significantly improved in large-EPCs transplantation groups only (Figure 9C) compared with those of small-EPC, EC, or PBS transplantation groups. Moreover, immunohistochemical analysis clearly showed that capillary density in large-EPC transplantation groups was markedly increased (Figure 9D and E), suggesting that large-EPC-CFUs are more functional EPC status for vascular regeneration *in vivo*.

A

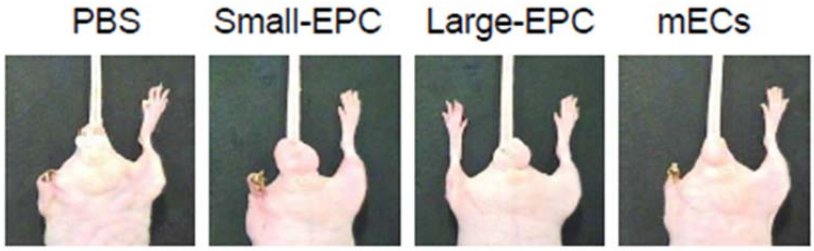
PBS
Small-EPC
Large-EPC
mECs

B

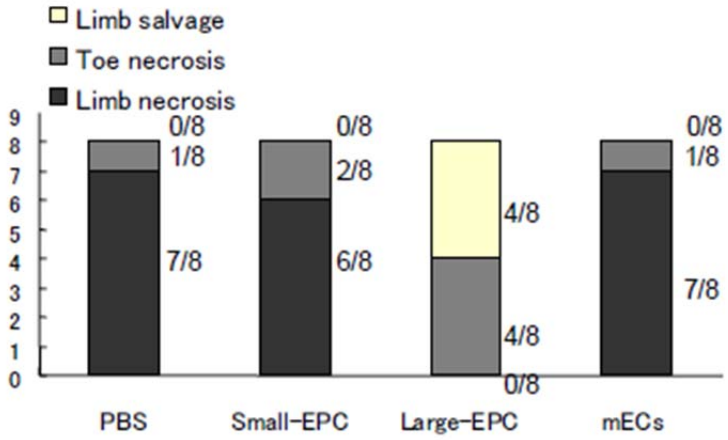
Limb salvage
Toe necrosis
Limb necrosis
9
8
7
6
5
4
3
2
1
0
0/8
1/8
7/8
0/8
2/8
6/8
4/8
4/8
0/8
0/8
1/8
7/8
PBS
Small-EPC
Large-EPC
mECs

C

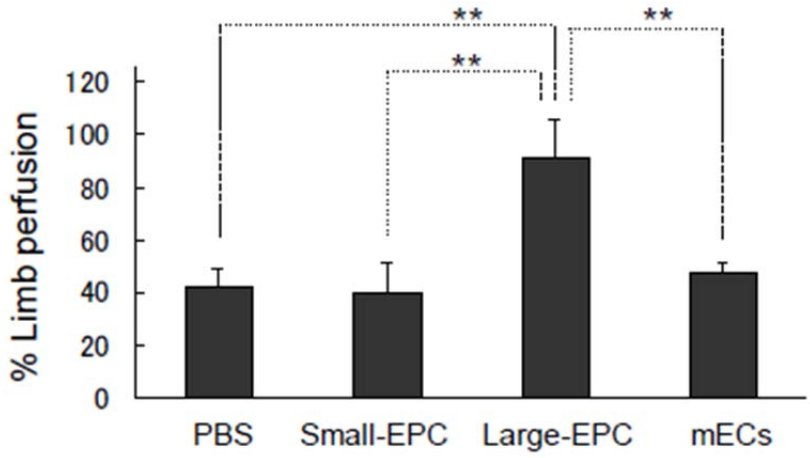
**
**
**
% Limb perfusion
120
100
80
60
40
20
0
PBS
Small-EPC
Large-EPC
mECs

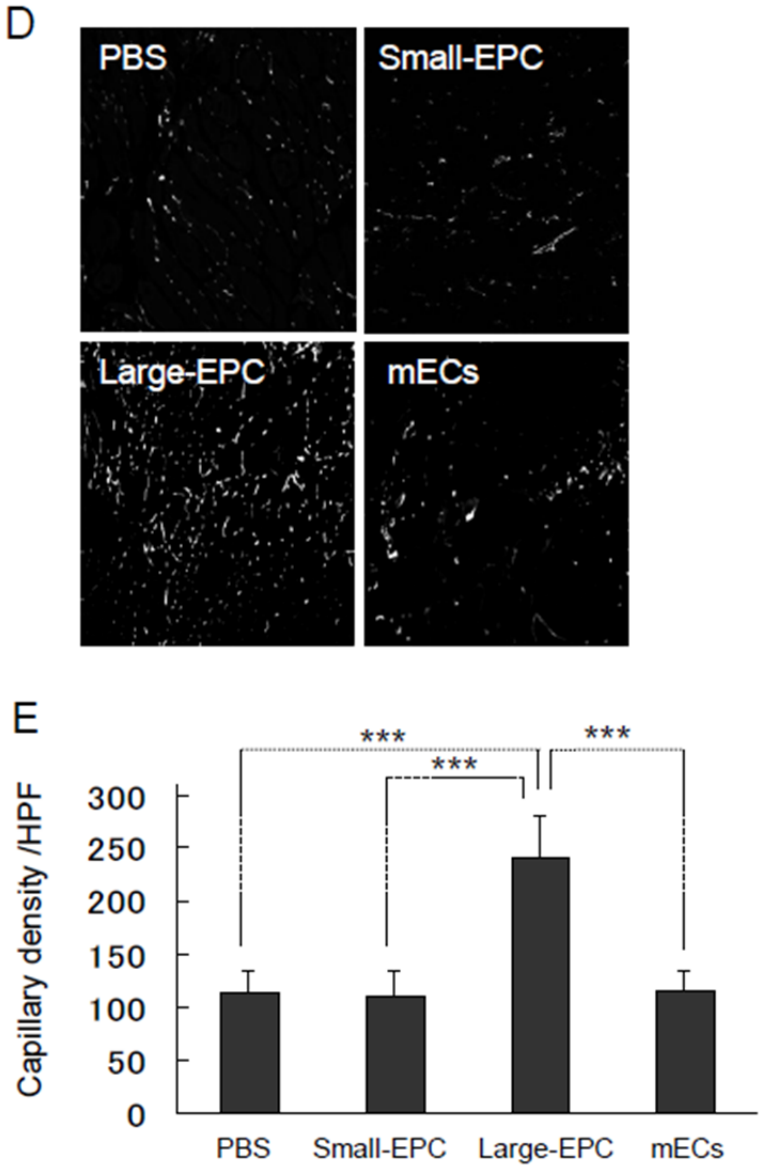

Figure 9　Effect of two types of EPC-CFUs on neovascularization.

A. Macroscopical observation of ischemic hindlimb 28 days after transplantation of large-EPCs and small-EPCs, which are derived from BM-KSL, and murine ECs into hindlimb ischemia. B. The ratios of the above outcomes in each group. C. Laser Doppler perfusion imaging showing reduction of blood flow at day 28 after surgery. Quantification data of blood flow as the ratio of perfusion in ischemic hindlimb to that in normal hindlimb are shown. In hindlimb ischemic mice, blood flow of hindlimb kept to be low in small-EPCs transplanted and other control groups at day 28 after surgery. Transplantation of large-EPCs recovered the limb perfusion in hindlimb ischemic mice. **P < 0.01 versus mice transplanted with large-EPCs (n = 8). D. Representative images of iso-lectin B4-positive tissue 28 days after transplantation of large-EPCs, small-EPCs, and mECs into

hindlimb ischemia. E. The statistical data of D. Transplantation of large-EPC into hindlimb ischemia model enhanced neovascularization. ***P < 0.001 versus mice transplanted with large-EPCs (n = 8). HPF, high-powered field.

2.4 Discussion

EPCs can be classified into various differentiation levels in both circulating EPCs and tissue EPCs [16]. Here, *in vivo* EPC status was defined by establishing the novel murine EPC-CFA, in which the colony-forming potential of EPCs at different differentiation levels can be assessed. It was demonstrated, for the first time, that hindlimb ischemia induced onsets of large-EPCs, which might be the accelerated differential status of EPCs. The observation was further supported by an *in vivo* experiment in which transplantation of more mature large-EPCs into a hindlimb ischemia model enhanced neovascularization, implying the contribution of large-EPC-CFUs in a pathogenic situation as 'cells ready to operate'.

Previously, Hur and colleagues [20] reported that they found two types of EPCs - early EPCs and late EPCs - from a source of adult PB-MNCs; attached cells that appeared after 3 to 5 days of culture were defined as early EPCs, and cells that appeared in 2 to 4 weeks after plating were defined as late EPCs [20]. However, these classifications gave us some limitation for a full understanding of the EPC status. First, as these two types of EPCs were defined by different assays, two types of EPCs could not be assayed synchronously. Second, these assays failed to provide enough information about the differential cascade from immature stem cells, such as BM-KSL, into real EPC status. In this study, EPC status in response to a pathogenic situation was redefined. Small-EPC-CFUs had greater proliferative activity, suggesting that small-EPC-CFUs contained more immature clonogenic cells (KSL cells) derived from hematopoietic stem cells which preserve hemagioblastic potentials. Large-EPC-CFUs are sequentially differentiated from small-EPC-CFUs in response to ischemic signals (Figure 10). That is, small-EPC-CFUs are 'primitive EPCs' and large-EPC-CFUs are 'definitive EPCs'. Importantly, in regard to the vasculogenic potential *in vivo*, this study clearly demonstrated that transplantation of definitive EPCs (large-EPCs), not primitive EPCs (small-EPCs), markedly increased limb perfusion and capillary density and that small-EPC-CFUs have pro-vasculogenic potential and large-EPC-CFUs have vasculogenic potential, although early and late EPCs were reported to contribute equally to neovasculogenesis in a previous study [20]. Regarding the fact that small-EPCs did not show any therapeutic effect in Figure 9, three possibilities were speculated due to the low adhesion and incorporation potentials of small-EPCs: (a) transplanted small-EPCs could not survive in a hypoxic tissue environment, (b) transplanted small-EPCs could not differentiate into large-EPCs in a hypoxic tissue environment, and (c) transplanted small-EPCs could not show their function as secretion of growth factors in a hypoxic tissue environment.

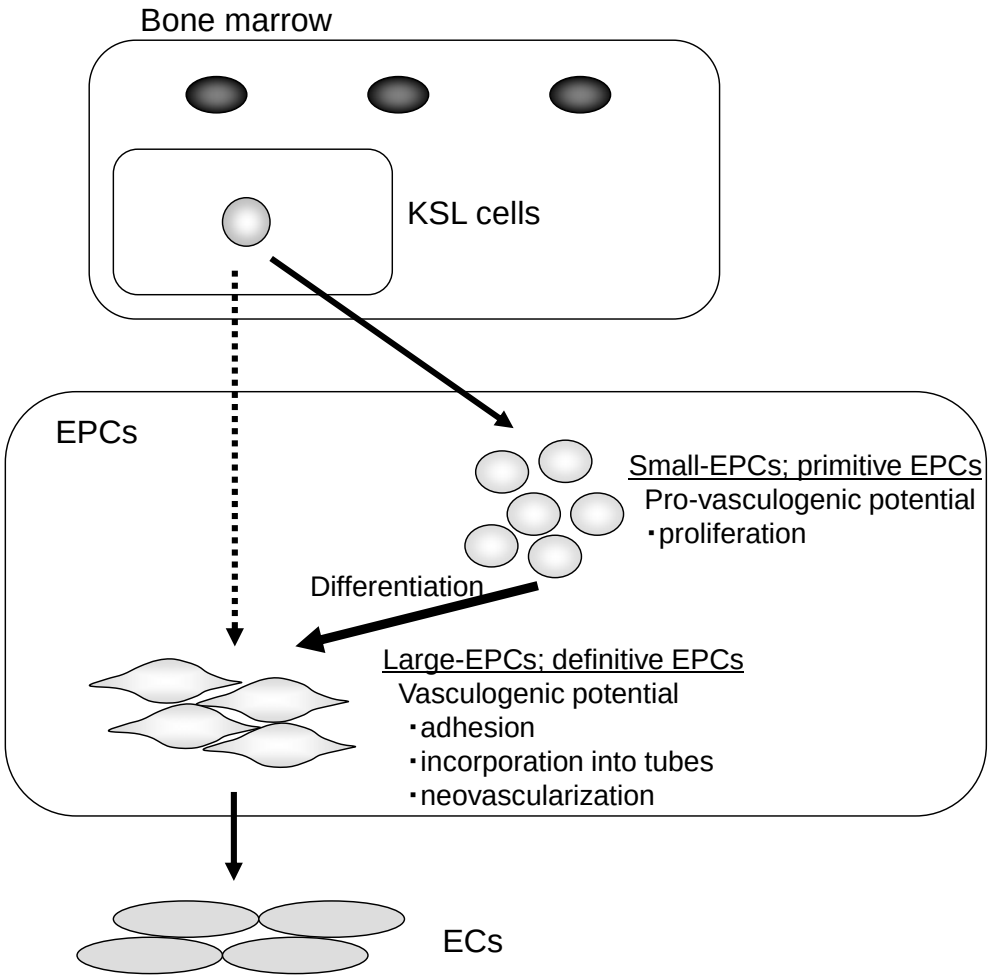

Figure 10　Schematic model of EPC development.

In an EPC-CFA, three different stages of EPC development were classified: (1) stem cell stage as EPC-sprouting cells, (2) early stage of EPCs as large-EPC-CFU-sprouting cells, which contained mostly immature small cells, and (3) late stage of EPCs as functional EPCs, which contained mostly big spindle cells.

Two types of EPC-CFUs represented distinct functional differences in both *in vitro* EPC colony study and *in vivo* EPC transplantation study. The adhesive potential and the incorporation into tubes formed by EC-like cells of large-EPCs were superior to those of small-EPCs, and small-EPCs had higher proliferation capacity than large-EPCs, which was consistent with the data on EPC-CFUs from BM-LNneg and BM-KSL (data not shown). In these points, definitive large-EPCs had similar functions to ECs compared with primitive small-EPCs. Besides, the secondary culture revealed that small-EPCs could differentiate into adherent cells, large-EPCs; in contrast, large-EPCs could not differentiate into round cells, small-EPCs (data not shown). These data showed that definitive

large-EPCs are well-differentiated EPCs compared with primitive small-EPCs. VE-cadherin is specifically expressed in adherent junctions of ECs and exerts important functions in cell-cell adhesion [33]. The different expression level of VE-cadherin between large-EPCs and small-EPCs might explain the better potential of adhesion, incorporation into tubes, and migration (data not shown) of definitive large-EPCs than those of primitive small-EPCs, which were consistent with the findings using human cord blood AC133(+) cells [34]. Gene expression profiles revealed that both EPC-CFUs were committed to endothelial lineage because both definitive large-EPCs and primitive small-EPCs expressed eNOS, Flk-1, and VE-cadherin, which are EC-specific markers [5]. However, both EPC-CFUs would be different from mature ECs in terms of colony formation capacity, tubular formation ability, and contribution of *in vivo* neovascularization, demonstrated by ischemia model, because ECs could not form colonies and did not have an effect on the restoration of blood vessels, and EPC-CFU-derived cells could not form tubes on Matrigel in a culture without ECs.

In this EPC-CFA, to compare the potentials to produce EPC-CFUs of three populations in BM (BM-MNCs, BM-LNneg, and BM-KSL), the numbers of cells producing one EPC-CFU was calculated in BM-MNC, BM-LNneg, and BM-KSL populations. It was revealed that one large-EPC-CFU was derived from $1.1 \times 10^3 \pm 0.2 \times 10^3$ BM-MNCs or $3.6 \times 10^2 \pm 1.1 \times 10^2$ BM-LNneg or 57 ± 34 BM-KSL (shown in Figure 7B). One small-EPC-CFU was derived from $5.5 \times 10^2 \pm 0.7 \times 10^2$ BM-MNCs or $1.2 \times 10^2 \pm 0.2 \times 10^2$ BM-LNneg or 28 ± 3 BM-KSL (shown in Figure 7B). These data demonstrated that BM-LNneg had 3- or 4.6-fold higher potential to produce large- or small-EPC-CFUs than BM-MNCs, respectively, and this suggested that more immature EPCs were contained mainly in the BM-LNneg population. In addition, it was demonstrated that BM-KSL had the highest potential to produce EPC-CFUs in any other populations in BM, and those potentials to produce large- or small-EPC-CFUs were 6.3- or 4.3-fold higher than BM-LNneg, respectively, and this suggested that immature EPCs were highly enriched in the BM-KSL population. In this study, using EPC-CFA, it was determined that BM-KSL was the major population which highly enriched immature EPCs. Furthermore, it was concluded that small-EPCs differentiated into large-EPCs because BM-KSL grew into small-EPCs about 5 days after plating and then those small-EPCs derived from BM-KSL could differentiate into large-EPCs in further culture. However, it remained unclear "which niche component does small- or large-EPC differentiate from". This should be definitely addressed in further issues.

In a clinical setting, the frequency of circulating EPCs serves as a biomarker for vascular function, and the number of circulating EPCs has been reported to be reduced in patients with diabetes mellitus or risk factors for coronary artery disease and to negatively correlate with the Framingham cardiovascular risk score [12-15]. Transplantation of EPCs into ischemic hindlimb or myocardial tissue improves organ function following new vessel growth [6-10]. Thus, EPCs play an important

role in the restoration of ischemic vascular diseases. But essential molecular events that control the differentiation to EPCs and changes in EPCs in response to ischemia had not been clarified yet. Then the changes of EPCs in response to hindlimb ischemia were investigated in EPC-CFA and it was revealed that the population of KSL, which enriched immature EPC populations in BM, increased by ischemia. In previous studies, it was demonstrated that BM-derived EPCs were mobilized in response to tissue ischemia [31]. In this study, it was showed, for the first time, that the ischemic signals could promote the differentiation of PB-MNCs, BM-MNCs, BM-LNneg or BM-KSL cells into mature EPC-CFUs. Ischemia-induced differentiation into large-EPC-CFUs suggested that definitive large-EPC-CFUs as more mature EPCs might play an important role in the restoration of ischemic tissue, and this possibility was supported by the recovery of limb perfusion by transplantation of BM-KSL-derived large-EPCs into a hindlimb ischemia model compared with small-EPCs. In ischemic tissue, the expression of stromal cell-derived factor-1 (SDF-1) was induced by transcription factor hypoxia-inducible factor-1 (HIF-1) according to hypoxic gradients [32,33]. SDF-1 enhances differentiation of BM-derived c-Kit+ stem cells into EPCs [34]. Thus, the EPC differentiation presented above might be promoted by SDF-1, which is induced by HIF-1 after ischemia.

In this chapter, the EPC-CFA has been established and could be a useful way to investigate the differentiation levels of murine EPCs, further providing a crucial clue that large-EPC-CFU status may be more functional or effective EPCs to promote neovascularization. In the next chapter, to elucidate the development and mechanical dysfunction of EPCs in T2D, the colony-forming capacity of EPCs and differentiation potential of BM-KSL were examined in T2D mice, *db/db* mice and *KKAy* mice, using newly established EPC-CFA.

3. Impaired development and dysfunction of endothelial progenitor cells in type 2 diabetic mice.

3.1 Purpose

In this chapter, to elucidate the development and mechanical dysfunction of EPCs in T2D, the colony-forming capacity of EPCs and differentiation potential of BM-KSL were examined in T2D mice, *db/db* mice and *KKAy* mice, using EPC-CFA established in the previous chapter. As BM-KSL have the plasticity to transdifferentiate into various cell types and given the close link established between the pathogenesis of T2D and inflammation, this study concomitantly investigated both the differentiation of BM-KSL into haematopoietic cells and development of vascular lineage cells in T2D mice. The results and new insights on differentiation into large-EPC-CFUs or GMs from BM-KSL in type 2 diabetic mice are described below.

3.2 Materials and methods

3.2.1 Animals

Experiments were performed with male 9- to 11-week-old *db/+* and *db/db* mice, and male 10- to 11-week-old C57BL/6J and *KKAy* mice (CLEA Japan, Inc., Tokyo, Japan), which were maintained under a 12-h light/dark cycle and in accordance with the regulations of Tokai University. Standard laboratory chow and water were available ad libitum. Mean body weight and blood glucose levels of the *db/+*, *db/db*, C57BL/6J and *KKAy* mice were, respectively: *db/+*: 28.0 ± 1.0 g and 142 ± 39 mg/dL; *db/db*: 44.5 ± 2.6 g and 356 ± 52 mg/dL ($P < 0.01$ versus *db/+* mice for both); C57BL/6J: 24.4 ± 0.6 g and 155 ± 34 mg/dL; and *KKAy*: 41.4 ± 3.3 g and 384 ± 68 mg/dL ($P < 0.01$ versus C57BL/6J mice for both).

3.2.2 Isolation of PB-MNCs and BM-KSL

Peripheral blood was obtained from the heart immediately before sacrifice and separated by Histopaque-1083 (Sigma-Aldrich, St. Louis, MO, USA) density gradient centrifugation, as previously described [30]. Briefly, low-density mononuclear cells were harvested and washed twice with Dulbecco's PBS, supplemented with 2 mmol/L EDTA. Contaminated red blood cells were haemolyzed using an ammonium-chloride solution.

BM-MNCs were obtained by flushing the femurs and tibias. Cells were exposed to a reaction mixture of biotinylated monoclonal antibodies (BD Biosciences, San Jose, CA, USA) against B220 (RA3-6B2), CD3 (145-2C11), CD11b (M1/70), TER-119 (Ly-76) and Gr-1 (RB6-8C5), used as lineage markers to deplete lineage-positive cells from BM-MNCs, with an autoMACS cell-separator system (Becton Dickinson, Franklin Lakes, NJ, USA). BM-LNneg were incubated with saturating concentrations of directly labelled anti-c-Kit, anti-Sca-1 and anti-CD34 antibodies (all from BD Biosciences) for 30 min on ice. The BM-KSL or CD34(+) BM-KSL or CD34(–)

BM-KSL were then isolated by live sterile cell-sorting (FACSVantage SE flow cytometry system; Becton Dickinson).

3.2.3 Endothelial progenitor cell culture assay *in vitro*

Modified EPC culture assay was performed as previously described [22]. In brief, BM-KSL (1×10^4 cells/well) were cultured in serum-free endothelial basal medium (EBM)-2 (Cambrex Bio Science Walkersville, Walkersville, MD, USA) with rat plasma vitronectin (Sigma-Aldrich) in a 0.5% gelatin solution and a 96-well plate (BD Biosciences). Four days after culture, cells were washed twice and incubated at 37 °C for 3 h in a medium containing 10 μg/mL acLDL-DiI (Biomedical Technologies Inc., Stoughton, MA, USA) and 20 μg/mL of FITC-conjugated BS-1 lectin (Sigma-Aldrich). After washing, cells were examined by fluorescence microscopy, with acLDL-DiI and BS-1 lectin double-positive cells counted in at least four separate, randomly selected, high-power fields.

3.2.4 Endothelial progenitor cell colony-forming assay

EPC-CFA was performed as previously described in 2.2.3. Briefly, cells were cultured in a methylcellulose-containing medium (MethoCult™ SF M3236, StemCell Technologies, Vancouver, BC, Canada) with 20 ng/mL stem cell-derived factor (Kirin-Sankyo Co. Ltd, Tokyo, Japan), 50 ng/mL vascular endothelial growth factor (R&D Systems, Inc., Minneapolis, MN, USA), 20 ng/mL interleukin-3 (Kirin-Sankyo), 50 ng/mL basic fibroblast growth factor (Wako, Osaka, Japan), 50 ng/mL epidermal growth factor receptor (Wako, Osaka, Japan), 50 ng/mL insulin-like growth factor-1 (Wako), 2 U/mL heparin (Ajinomoto Co., Inc., Tokyo, Japan) and 10% FBS in a 35-mm dish for 8 days. Cell densities for each sample were: PB-MNCs: 7×10^5 cells/dish; BM-KSL: 500 cells/dish; and CD34(+) or CD34(–) BM-KSL: 500 cells/dish. EPC-CFUs were identified as large-EPC-CFUs or small-EPC-CFUs by visual inspection, using an inverted microscope under × 40 magnification. Large-EPC-CFUs were mainly composed of spindle-shaped cells and small-EPC-CFUs comprised round cells.

3.2.5 Haematopoietic colony-forming assay

BM-KSL (500 cells/dish) were cultured in MethoCult™ GF M3434 (StemCell Technologies, Vancouver, BC, Canada) in a 35-mm dish for 7 days. Haematopoietic CFUs were identified as GMs by visual inspection by an inverted microscope under × 40 magnification. CFU-GM colonies often contain multiple cell clusters comprising monocytic lineage cells, large cells with an oval-to-round shape and an apparently grainy or grey centre, and granulocytic lineage cells, which are round, bright, and much smaller and more uniform in size than macrophage cells.

3.2.6 Endothelial progenitor cell colony-forming unit staining

After 8 days, the CFU cultures were treated with 0.4 μg/mL acLDL-DiI for 1 h and fixed by the application of 1 mL 2% paraformaldehyde for 1 h at room temperature. After washing the methylcellulose-containing medium with PBS, the cultures were reacted with FITC-conjugated BS-1 lectin for 1 h at room temperature. After washing again with PBS, the cultures were examined by fluorescence microscopy (IX70, Olympus Corporation, Tokyo, Japan).

3.2.7 Flow cytometry

For this analysis, monoclonal antibodies specific to Sca-1, c-Kit, CD34 and CD11b were used. BM-LNneg cells were incubated with directly labelled anti-Sca-1, anti-c-Kit and anti-CD34 antibodies for 30 min on ice. BM-MNCs and PB-MNCs were incubated with biotin-conjugated anti-CD11b antibody for 30 min on ice. Cells were then washed and incubated with FITC-conjugated streptavidin for 30 min on ice, then analyzed by FCM using a FACSCalibur (Becton Dickinson).

3.2.8 Proliferation assay of BM-KSL

The *db/+* and *db/db* mice were injected intraperitoneally with BrdU (100 mg/5 mL/kg, Sigma-Aldrich) or saline as a control; BM-KSL were then prepared 18 h later. After isolation, BM-LNneg cells were stained for c-Kit, Sca-1 and BrdU (anti-BrdU-FITC), according to the BrdU Flow Kit manual (BD Biosciences).

3.2.9 Statistical analysis

All data are presented as means ± SD. P values were calculated using the unpaired Student t-test, and $P < 0.05$ was considered statistically significant.

3.3 Results

3.3.1 Impaired stem/progenitor cell population in bone marrow of *db/db* mice

Because circulating EPCs originate from stem cells in BM, the stem/progenitor cell population was measured first for KSL cells in *db/db* mice. FCM analysis revealed that the percentage of the KS population in BM-LNneg in *db/db* mice was significantly decreased (2.2 ± 0.5%) compared with levels in *db/+* mice (4.7 ± 0.9%; Figure 11A and B). To investigate the proliferation capacity of stem/progenitor cells in *db/db* mice, BrdU analysis was performed. After incorporation *in vivo* of BrdU for 18 h in BM-KSL, the percentage of BrdU-positive BM-KSL was significantly decreased in *db/db* mice compared with *db/+* mice (42.7 ± 3.4% and 62.9 ± 7.8%, respectively; Figure 11C and D). These findings suggest that T2D might have an effect on stem/progenitor cells, a source of EPCs, by regulating the proliferation cascade in *db/db* mice, thus also possibly explaining EPC

dysfunction.

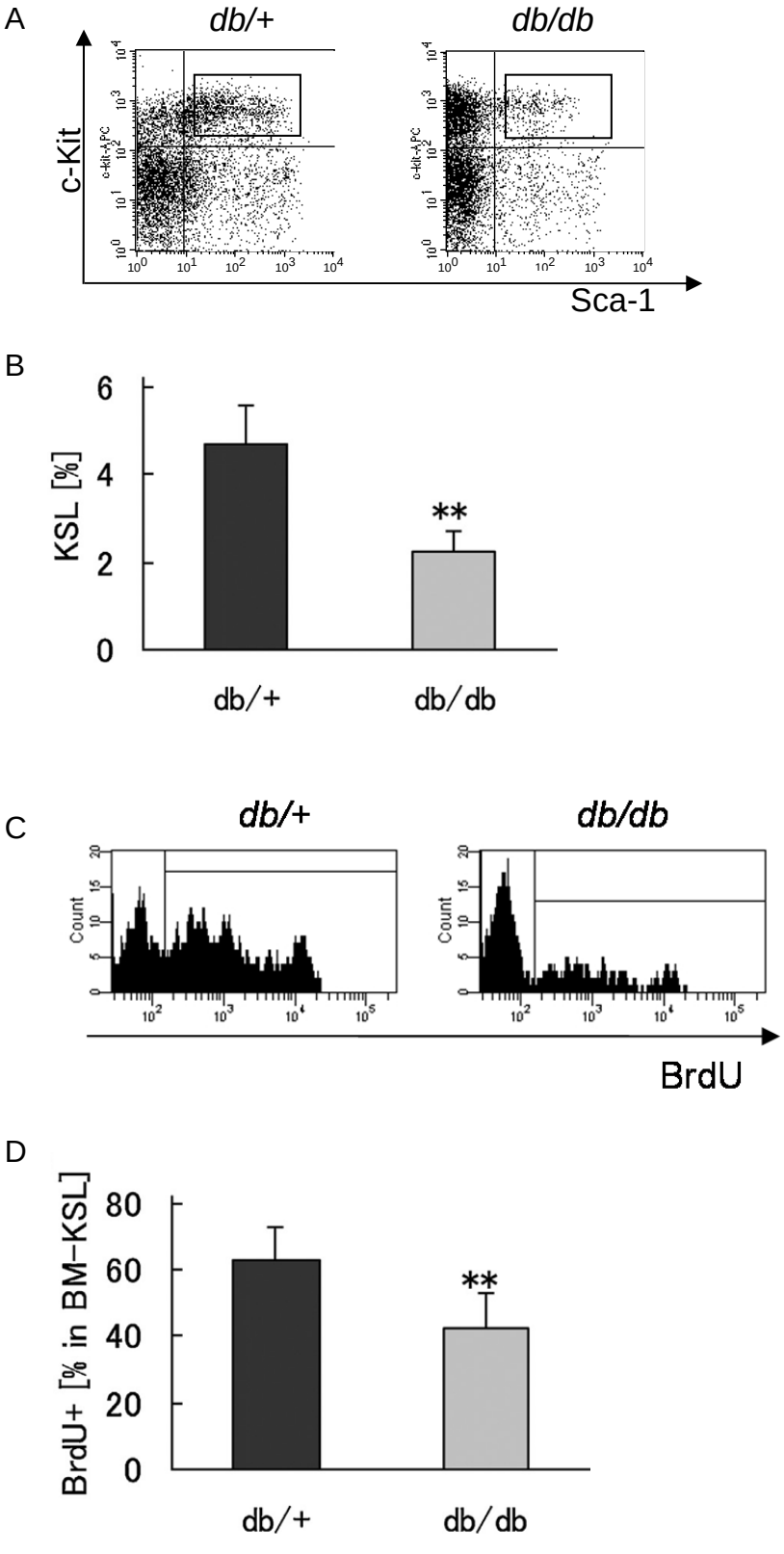

Figure 11　Impaired stem/progenitor cell population in the BM of *db/db* mice.

A. FCM analysis of BM-LNneg in *db/+* and *db/db* mice using rat IgG antibodies against mouse c-Kit and Sca-1. B. Percentage of the KSL population in BM-LNneg was decreased in *db/db* mice. **P < 0.01 versus *db/+* mice. C. *In vivo* (18-h) proliferation of BM-KSL in *db/+* and *db/db* mice analyzed by FCM following administration of BrdU or saline. D. Quantification (%) of BrdU incorporated into BM-KSL shows a significantly lower proliferation capacity in *db/db* mice. **P < 0.01 versus *db/+* mice.

3.3.2　Specific regulation of endothelial progenitor cell development in *db/db* mice

To investigate the differentiation potential of BM-KSL into EPCs, the numbers of EPCs differentiated from BM-KSL were assessed by EPC culture assay using acLDL-DiI uptake and BS-1 lectin reactivity (Figure 12A and B). A significant decrease was observed in the potential of EPC differentiation in T2D *db/db* mice compared with normal *db/+* mice (20.9 ± 3.5 cells/field and 32.6 ± 3.7 cells/field, respectively; Figure 12C).

Next, the capacity of BM-KSL to form EPC-CFUs was assessed by EPC-CFA. In chapter 2, it was reported that BM-KSL could differentiate into either small-EPC-CFUs (immature EPCs) or large-EPC-CFUs (mature EPCs), and both types of CFUs differentiated from primary BM-KSL were identified as EPCs by acLDL-DiI uptake and BS-1 lectin reactivity (Figure 12D and E). The frequency of large-EPC-CFUs differentiated from the BM-KSL of *db/db* mice was significantly decreased (7.2 ± 2.6 per dish) compared with *db/+* mice (10.6 ± 2.2 per dish). In contrast, there was no significant difference between the frequencies of small-EPC-CFUs from *db/+* and *db/db* mice (Figure 12F). These results demonstrate that the capacity to form large-EPC-CFUs and mature EPCs was specifically decreased in the BM-KSL of T2D *db/db* mice, suggesting an impaired differentiation potential. The predicted frequencies of both large-EPC-CFUs and small-EPC-CFUs derived from 1×10^5 BM-MNCs were significantly decreased in *db/db* mice, which have BM-KSL impairment not only in number, but also in differentiation potential (Figure 12G).

A

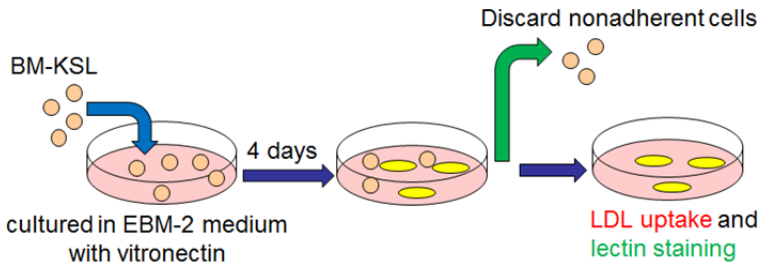
Discard nonadherent cells
BM-KSL
4 days
cultured in EBM-2 medium
with vitronectin
LDL uptake and
lectin staining

B

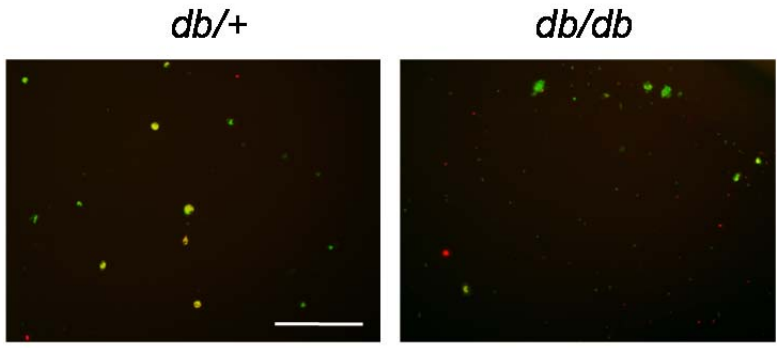
db/+
db/db

C

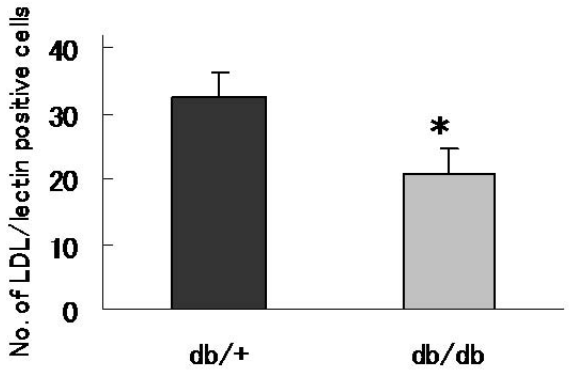
No. of LDL/lectin positive cells
40
30
20
10
0
*
db/+
db/db

D

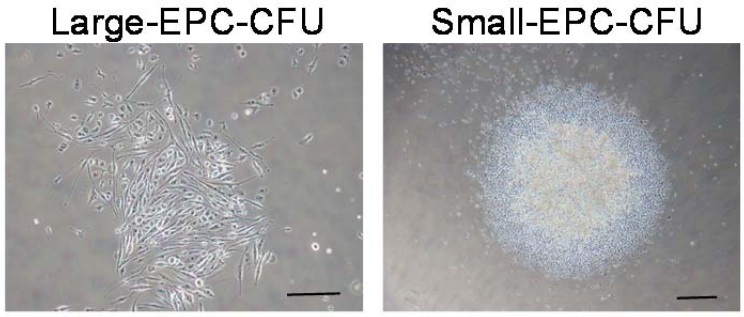
Large-EPC-CFU
Small-EPC-CFU

E

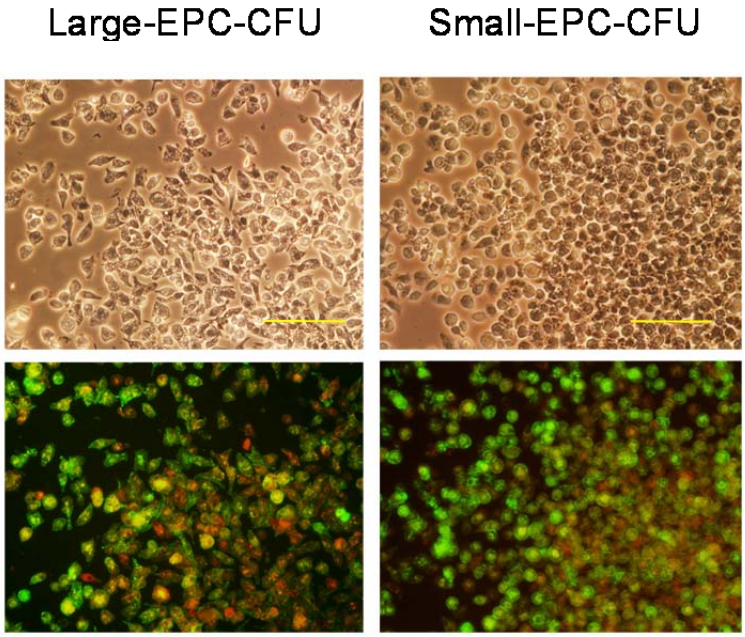
Large-EPC-CFU
Small-EPC-CFU

F

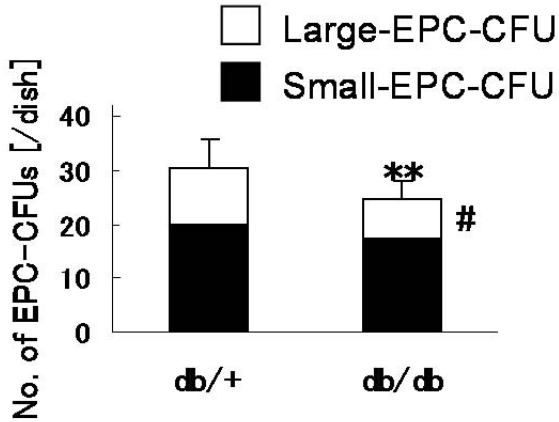
Large-EPC-CFU
Small-EPC-CFU
No. of EPC-CFUs [/dish]
40
30
20
10
0
**
#
db/+
db/db

G

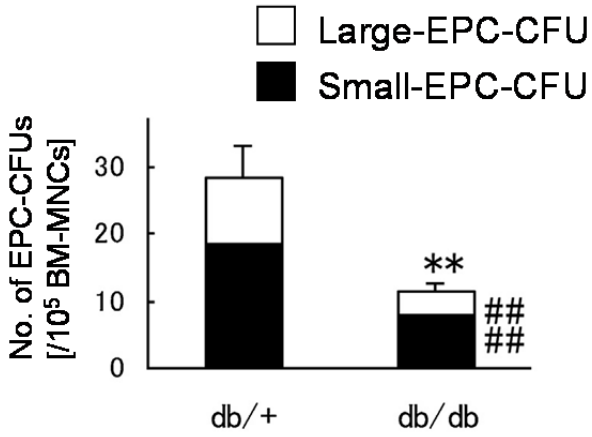
Large-EPC-CFU
Small-EPC-CFU
No. of EPC-CFUs [/10⁵ BM-MNCs]
30
20
10
0
**
##
##
db/+
db/db

Figure 12　Specific regulation of EPC development in *db/db* mice.

A. Schematic of EPC culture assay protocol. B. Representative fluorescence photomicrographs of EPCs from BM-KSL in *db/+* and *db/db* mice after 4 days of culture: EPCs appear as double-positive cells due to acLDL-DiI uptake (red) and BS-1 lectin reactivity (green); scale bar = 500 μm. C. EPC culture assays of BM-KSL from *db/+* and *db/db* mice show that EPCs are less differentiated in *db/db* mice than in *db/+* mice. *P < 0.05 versus *db/+* mice. D. Representative micrographs of large-EPC-CFUs and small-EPC-CFUs cultured from BM-KSL of *db/+* mice for 8 days show they can be identified by cell morphology (spindle-shaped and round cells, respectively); scale bar = 250 μm (left) and 500 μm (right). E. CFUs can be identified as double-positive cells because of acLDL-DiI uptake (red) and BS-1 lectin reactivity (green); scale bar = 100 μm. F. EPC-CFAs of BM-KSL in *db/+* and *db/db* mice show frequencies of large-EPC-CFUs (white columns) and small-EPC-CFUs (black columns), respectively, after 8 days of culture: *db/db* mice had dysfunctional large-EPC-CFU formation and EPC developmental potential. **P < 0.01 versus total CFUs from *db/+* mice, #P < 0.05 versus large-EPC-CFUs from *db/+* mice. G. Quantification of the predicted number of large-EPC-CFUs and small-EPC-CFUs differentiated from 1×10^5 BM-MNCs in *db/+* and *db/db* mice. **P < 0.01 versus total CFUs from *db/+* mice, ##P < 0.01 versus large-EPC-CFUs and small-EPC-CFUs from *db/+* mice.

In peripheral blood, the frequency of large-EPC-CFUs differentiated from primary PB-MNCs of *db/db* mice was significantly decreased compared with *db/+* mice, and the frequency of total CFUs was also decreased (Figure 13A and B). These results demonstrate that the potential to differentiate into mature EPCs and form EPC-CFUs was also attenuated in peripheral blood from T2D *db/db* mice, supporting the hypothesis that *db/db* mice have a dysfunction of EPC development in BM.

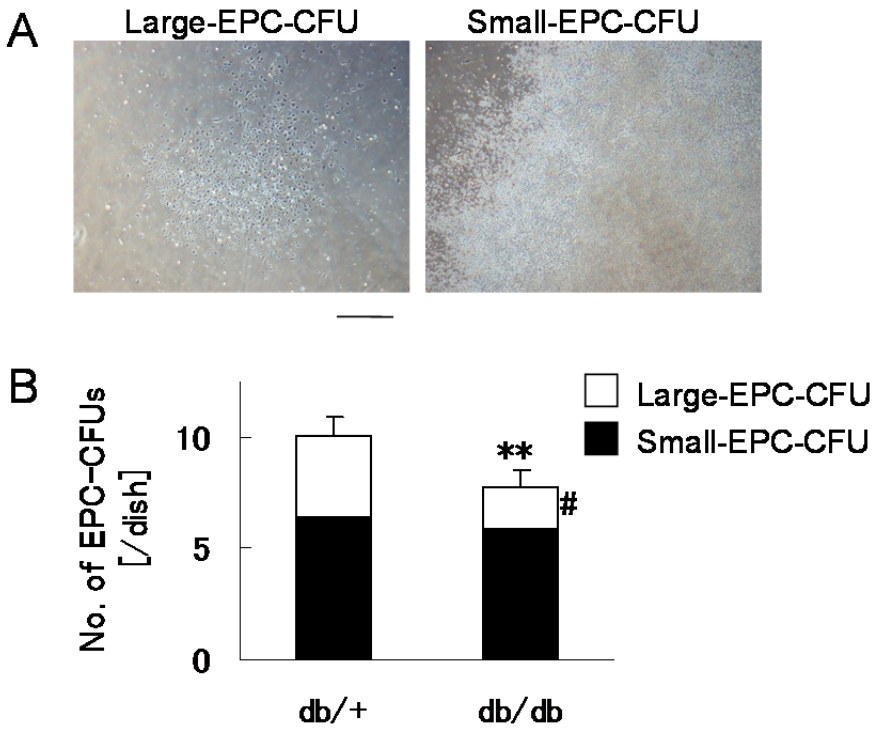

Figure 13 EPCs in peripheral blood from *db/db* mice.

A. Representative micrographs of large-EPC-CFUs and small-EPC-CFUs cultured from PB-MNCs of *db/+* mice for 8 days; scale bar = 1 mm. B. Results of EPC-CFAs of PB-MNCs from *db/+* and *db/db* mice show frequencies of large-EPC-CFUs (white columns) and small-EPC-CFUs (black columns) after 8 days of culture. Fewer large-EPC-CFUs were differentiated from PB-MNCs in *db/db* mice. **P < 0.01 versus total CFUs in *db/+* mice, #P < 0.05 versus large-EPC-CFUs in *db/+* mice.

3.3.3 Endothelial progenitor cell development of BM-KSL in *db/db* mice

To further clarify the kinetics of BM-KSL in *db/+* and *db/db* mice, the population of CD34(+) cells in BM-KSL, which may be enriched in progenitor cells, was also examined. FCM analysis revealed that the percentage of CD34(+) cells in the BM-KSL of *db/db* mice was significantly decreased (53.7 ± 19.8%) compared with *db/+* mice (68.0 ± 12.2%; Figure 14A and B). Furthermore, on investigating the EPC differentiation capacities of both CD34(+) and CD34(–) BM-KSL in *db/+* and *db/db* mice, it was found that CD34(+) BM-KSL produced more EPC-CFUs and, in particular, differentiated into large-EPC-CFUs more than the CD34(–) BM-KSL (Figure 14C). The frequencies of large-EPC-CFUs differentiated from both CD34(+) and CD34(–) BM-KSL of *db/db* mice were significantly decreased compared with *db/+* mice (Figure 14C). These results demonstrate that the BM-KSL of *db/db* mice contain only a small number of CD34(+) cells, which

produce more EPC-CFUs than in CD34(-) cells, suggesting that the reduced CD34(+) BM-KSL in *db/db* mice may be contributing to their lower frequencies of total CFUs and large-EPC-CFUs.

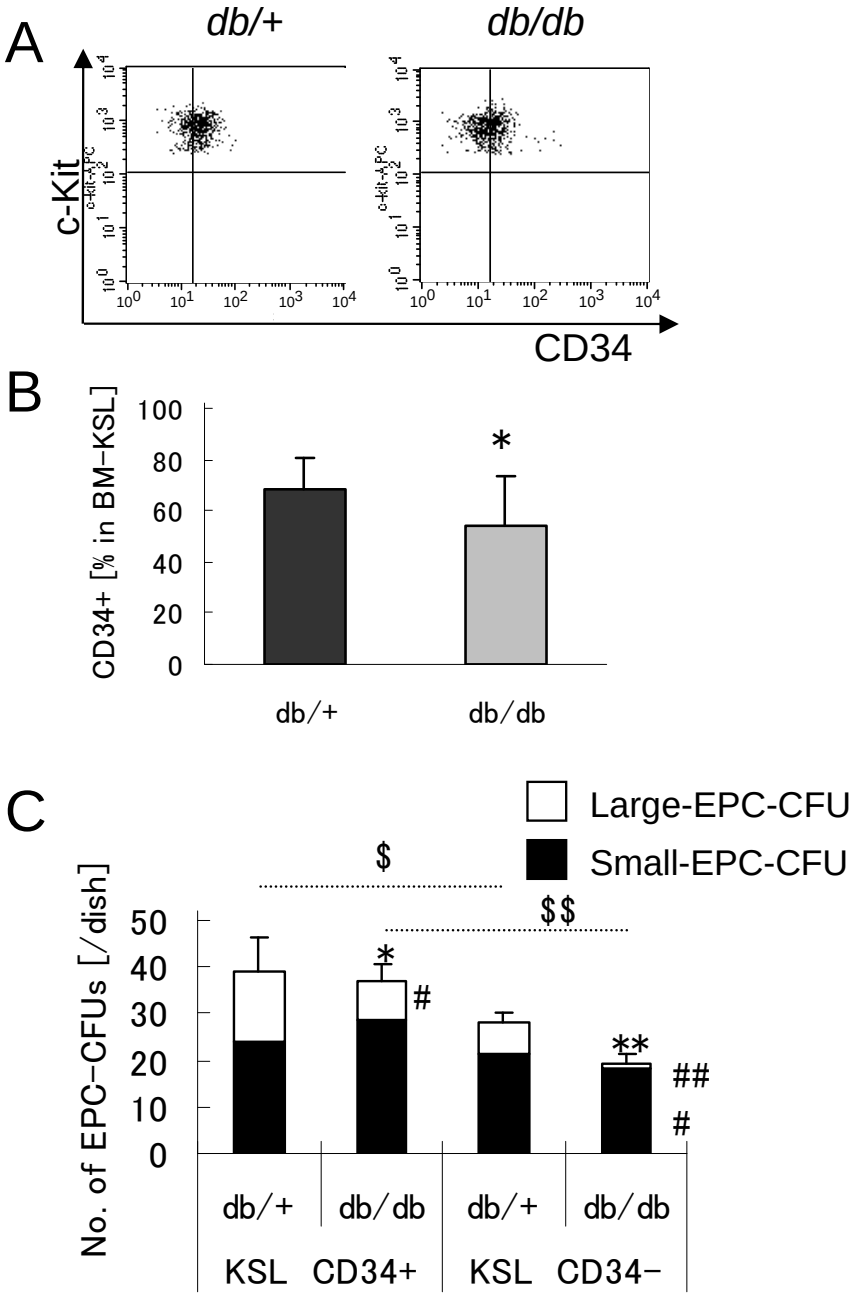

Figure 14　EPC development from BM-KSL in *db/db* mice.

A. FCM analysis of BM-KSL in *db/+* and *db/db* mice using rat IgG antibodies against mouse c-Kit, Sca-1 and CD34. B. Percentage of CD34(+) population in BM-KSL was decreased in *db/db* mice. *P < 0.05 versus *db/+* mice. C. EPC-CFAs of CD34(+) BM-KSL and CD34(–) BM-KSL from *db/+*

and *db/db* mice show frequencies of large-EPC-CFUs (white columns) and small-EPC-CFUs (black columns), respectively, following 8 days of culture. *P < 0.05 and **P < 0.01 versus total CFUs from CD34(+) and CD34(–) BM-KSL of *db/+* mice; #P < 0.05 and ##P < 0.01 versus large-EPC-CFUs and small-EPC-CFUs from CD34(+) and CD34(–) BM-KSL of *db/+* mice; $P < 0.05 and $$P < 0.01 versus total CFUs from CD34(+) and CD34(-) BM-KSL, respectively.

3.3.4 Differentiation potential of BM-KSL into granulocyte macrophages in *db/db* mice

Because BM-KSL have the plasticity to transdifferentiate into various cell lineages, including EPCs and haematopoietic cells, and as T2D has been reported to give rise to altered macrophage function [35-37], the capacity of BM-KSL to differentiate into GMs was examined. On haematopoietic CFA, BM-KSL were found to differentiate into GM-CFUs, and the frequency in *db/db* mice was significantly increased to 135 ± 10 CFUs/dish compared with 107 ± 10 CFUs/dish in *db/+* mice (Figure 15A-C). The percentage of BM CD11b(+) cells, a cell surface marker of monocytes, was also significantly increased in *db/db* mice compared with *db/+* mice (13.1 ± 1.9% versus 9.1 ± 2.2%, respectively; Figure 15D). These results reveal that, in spite of the lower differentiation potential into EPCs, BM-KSL demonstrate a greater potential to differentiate into GMs in *db/db* mice than in *db/+* mice.

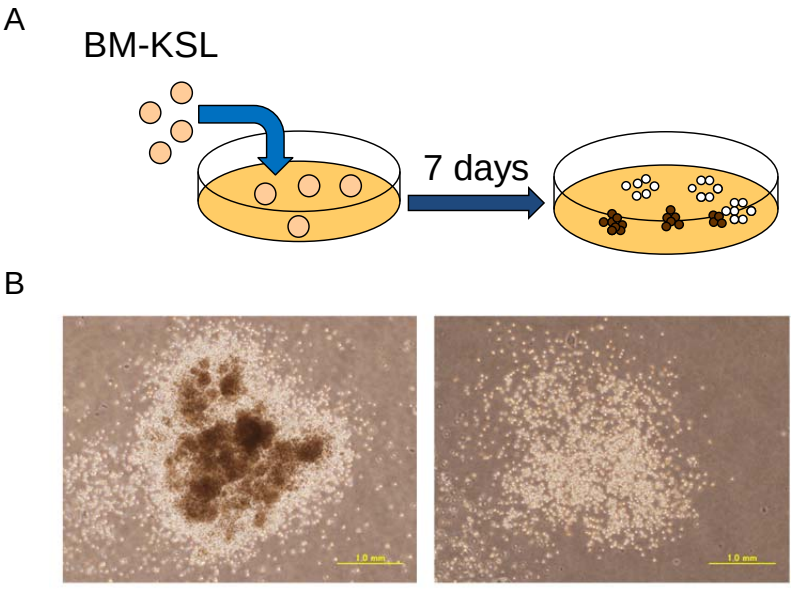

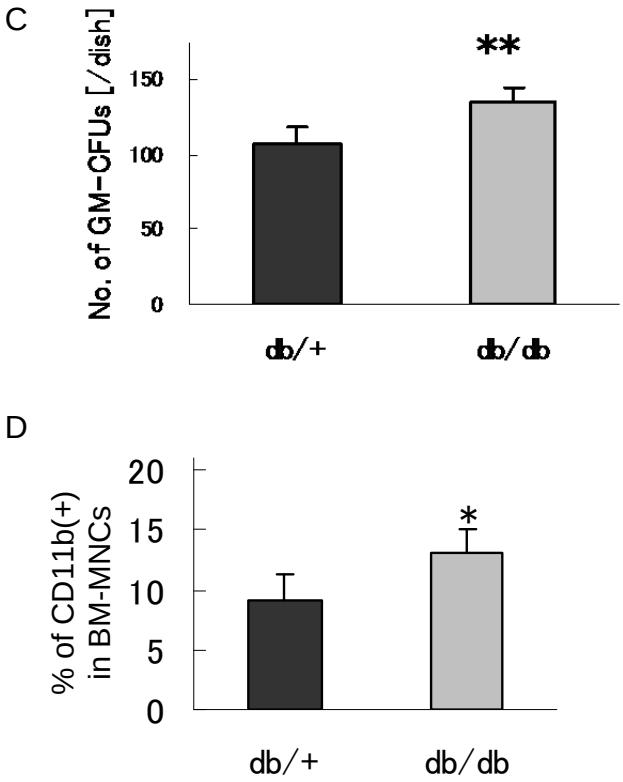

Figure 15　Differentiation potential of BM-KSL into GMs in *db/db* mice.

A. Schematic of haematopoietic CFA protocol. B. Representative micrographs of GM-CFUs cultured for 7 days from BM-KSL of *db/+* mice show GM colonies identified by cell morphology: GM-CFUs often contain multiple cell clusters of monocytic lineage cells and granulocytic lineage cells; scale bar = 1 mm. C. Haematopoietic CFAs of BM-KSL in *db/+* and *db/db* mice: frequencies of GM-CFUs were counted after 7 days of culture and revealed greater differentiation potential into GM in *db/db* mice. **P < 0.01 versus GM-CFUs from *db/+* mice. D. Percentage of CD11b(+) population in BM-MNCs was increased in *db/db* mice. *P < 0.05 versus *db/+* mice.

3.3.5　Endothelial progenitor cell development in type 2 diabetic *KKAy* mice

To determine whether EPC dysfunction in T2D *db/db* mice was caused by hyperglycaemia or a lack of leptin signalling, BM-KSL in *KKAy* mice, which are obese mice with T2D, was examined. In *KKAy* mice, the percentage of the KSL population in BM-LNneg was significantly decreased (1.9 ± 0.9%) compared with normal C57BL mice (5.6 ± 1.0%; Figure 16A), and there were also fewer CD34(+) cells in the BM-KSL than in C57BL mice (47.0 ± 8.1% and 63.0 ± 7.2%, respectively; Figure 16B). On EPC-CFA, the frequency of large-EPC-CFUs differentiated from the BM-KSL of *KKAy* mice was significantly decreased (6.5 ± 2.3 per dish) compared with that of C57BL mice (12.5 ± 2.9 per dish). In contrast, no significant difference was observed in the frequencies of small-EPC-CFUs between C57BL and *KKAy* mice (Figure 16C). On haematopoietic CFA,

BM-KSL was able to differentiate into GM-CFUs, and the frequency in *KKAy* mice was significantly increased (144 ± 14 CFUs/dish) compared with C57BL mice (119 ± 12 CFUs/dish; Figure 16D). These EPC and haematopoietic CFAs revealed that BM-KSL from *KKAy* mice had a lower potential to differentiate into large-EPC-CFUs in contrast to a greater potential to differentiate into GMs. These findings support the EPC dysfunction found in *db/db* mice and indicate that hyperglycemia, and not lack of leptin, is the most likely cause of the EPC and BM-KSL dysfunction in T2D mice.

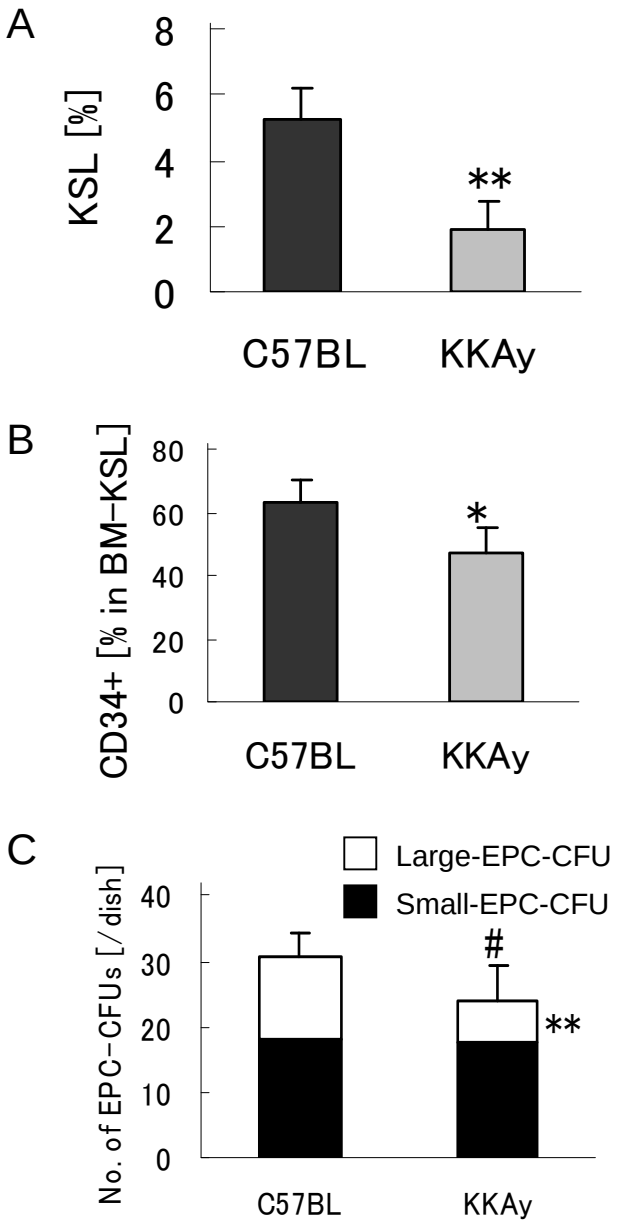

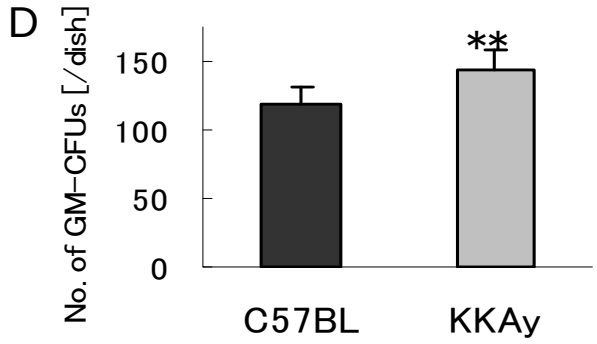

Figure 16　EPC development in T2D *KKAy* mice.

A. Percentages of KSL population in BM-LNneg from C57BL/6J and *KKAy* mice show a decreased BM-KSL population in *KKAy* mice on FCM analysis using rat IgG antibodies against mouse c-Kit and Sca-1. **P < 0.01 versus C57BL/6J mice. B. Percentages of CD34(+) population in BM-KSL from C57BL/6J and *KKAy* mice show a decreased CD34(+) population in *KKAy* mice using rat IgG antibodies against mouse c-Kit, Sca-1, and CD34. *P < 0.05 versus C57BL/6J mice. C. EPC-CFAs of BM-KSL from C57BL/6J and *KKAy* mice show frequencies of large-EPC-CFUs (white columns) and small-EPC-CFUs (black columns) after 8 days of culture. *KKAy* mice had dysfunctional large-EPC-CFU formation and impaired EPC differentiation potential. **P < 0.01 versus large-EPC-CFUs and #P < 0.05 versus total EPC-CFUs from C57BL/6J mice. D. Haematopoietic CFAs of BM-KSL from C57BL/6J and *KKAy* mice show frequencies of GM-CFUs after 7 days of culture and a greater potential to differentiate into GM in *KKAy* than in C57BL/6J mice. **P < 0.01 versus C57BL/6J mice.

3.4　Discussion

Microvascular diseases are common, severe complications of T2D, and such patients also have an increased risk of developing atherosclerotic disease and having poor outcomes after vascular occlusion [27,28]. Recently, accumulating evidence has reported that EPC dysfunction contributes to the pathogenesis of vascular complications in T2D [12,13,38,39]. In this study, it was demonstrated, using EPC-CFA, the dysfunctional differentiation of PB-MNCs and BM-KSL into more mature EPCs as well as dysfunctional colony formation of EPCs in *db/db* and *KKAy* mice. On the other hand, the differentiation of BM-KSL into GMs was promoted in these T2D mice. Thus, this study has demonstrated for the first time that T2D inhibits differentiation into vascular cells while promoting differentiation into haematopoietic cells, suggesting opposing mechanisms in the regulation of differentiation into EPCs and GMs in mice with T2D.

Circulating EPCs have the ability to differentiate into mature endothelium, and play a protective role against ischemia and atherosclerosis. Because circulating EPCs in peripheral blood are derived

from stem/progenitor cells in BM [40], this study focused on the BM-KSL of *db/db* mice. The percentage of BM lineage-negative cells was not affected by the diabetic state, and the percentage of BM-KSL in *db/+* mice was similar to that in normal C57BL/6J mice (data not shown). In *db/db* mice, the lower proliferation of BM-KSL may be contributory to the reduced KSL population. The BM-KSL, which are BM progenitors with highly enriched immature EPCs, were significantly reduced in number and function in T2D mice, suggesting that not only the process of mobilization, but also the central compartment was affected by the diabetic state. A reduced frequency of large-EPC-CFUs, described as mature EPCs with ongoing vasculogenic potential, was also shown from BM-KSL in *db/db* mice, again implying EPC dysfunction in differentiation and colony formation. As hind-limb ischemia can induce large-EPC-CFUs from BM-KSL in normal mice, EPC dysfunction in differentiation and colony formation in T2D might also be contributory to ischemic microvascular diseases. EPC-CFA has demonstrated that CD34(+) BM-KSL have greater potency in colony formation and differentiation into EPC-CFUs than CD34(–) BM-KSL. The decrease of CD34(+) BM-KSL in T2D mice, as observed by FCM analysis, reveals the inhibition of BM differentiation in such mice. Thus, the lower frequencies of BM-KSL-derived EPC-CFUs in T2D mice could be due to the reduced number of CD34(+) BM-KSL, which produce more EPC-CFUs than CD34(–) BM-KSL.

In addition, the reduced number of large-EPC-CFUs from PB-MNCs in *db/db* mice indicates a dysfunction of circulating EPC for differentiation and colony formation. Stromal-cell-derived factor-1 (SDF-1) is a critical chemokine for EPC recruitment to areas of ischaemia [32,41] and was reported to enhance differentiation into EPCs [34]. In T2D patients, EPCs derived from CD34(+) PB-MNCs demonstrated a marked defect in responding to SDF-1, as measured by the cell surface activity of CD26/dipeptidyl peptidase IV, an enzyme that inactivates SDF-1 [42]. This inability of diabetic EPCs to respond to SDF-1 might be contributing to the attenuation of EPC differentiation in T2D.

EPC and haematopoietic CFAs have revealed that mice with T2D have a dysfunction of differentiation of PB-MNCs and BM-KSL into more mature EPCs and EPC colony formation. In contrast, the differentiation capacity of BM-KSL into GMs was promoted in diabetic mice, suggesting that T2D inhibits differentiation into vascular cells, but promotes differentiation into haematopoietic cells. The upregulated differentiation into GMs in T2D mice is consistent with reports in type 1 diabetes non-obese diabetic (NOD) mice [43,44]. Recently, a close link between diabetes and inflammation was reported [45-48]. Macrophages from *db/db* mice exhibited altered function and expression of key inflammatory chemokines associated with the pathogenesis of diabetic vascular dysfunction and arteriosclerosis [35-37]. In this study, the percentage of CD11b(+) BM-MNCs was increased in *db/db* mice (Figure 15D). In addition, the percentage of the macrophage marker CD11b(+) in PB-MNCs was higher in *db/db* than in *db/+* mice (data not

shown). However, this increase could have been caused by the weak but constant inflammation and tissue injury seen in T2D mice.

The present study analyzed *db/db* mice as a well-characterized mouse model of T2D, with the development of hyperinsulinaemia, hyperglycaemia and insulin resistance [49,50] compared with their non-diabetic heterozygote littermates (*db/+* mice) as controls. Mice with *db/db* have a mutation in the leptin receptor gene, resulting in deletion of the cytoplasmic tail needed for intracellular signalling [50]. Therefore, it was relevant to clarify whether the reduced differentiation potential of the BM-KSL into EPCs and decreased CD34(+) BM-KSL population observed in *db/db* mice were caused by deletion of leptin signalling. For this reason, various experiments were performed with *KKAy* mice, transduced with the lethal yellow (*Ay*) mutation in the agouti gene as a model of T2D, which developed marked obesity with hyperglycaemia, hyperlipidaemia and hyperinsulinaemia [51]. The results obtained from *KKAy* mice were similar to those from *db/db* mice:

- a decrease in the BM-KSL population;
- a decrease in CD34(+) cells in BM-KSL;
- inhibition of differentiation into large-EPC-CFUs;
- promotion of differentiation into GMs.

Thus, the EPC dysfunction in the diabetic *db/db* and *KKAy* mice observed in this study were caused by impaired developmental and maturation signals of EPCs due to the multiple altered signal cascades of T2D. Previously, it was reported that *KKAy* mice showed renal lesions and decreased motor nerve conduction velocity similar to human diabetic nephropathy and neuropathy as diabetic complications [52]. This is the first report to confirm EPC dysfunction in *KKAy* mice.

The present study has clearly demonstrated a specific impairment in the development of EPCs in T2D. Elucidation of the mechanisms underlying these impairments could be helpful in the further development of therapies that work through recovery of BM or EPCs in microvascular and other ischemic diseases in such patients. Many studies of the transplantation of BM-MNCs from diabetic mice into wounds or ischemic limbs have demonstrated that the BM-MNCs of *db/db* mice inhibit neovascularization and fail to restore blood flow due to BM-MNC dysfunction [53,54]. Autotransplantation of recovered BM-MNCs or PB-MNCs into ischemic tissue in diabetic patients may provide therapeutic advantages in the efficacy of transplantation. EPC-CFA might be a useful way to analyze differentiation levels and the colony-forming potential of EPCs in many animal models, further providing crucial clues associated with pathological or pathogenic effects. Furthermore, the promotion of differentiation into GMs was revealed in T2D mice, implying opposing regulation of differentiation between EPCs and GMs (Figure 17). The various recent studies have provided evidence that inflammation, or the molecules and networks integral to inflammatory responses, are linked to the development of metabolic diseases as well as the

complications that emerge with obesity and T2D [45-48]. Thus, a thorough understanding of the developmental cascade of BM-MNCs into EPCs and macrophages in adipose, liver, pancreas and muscle tissues may yield a new strategy against diabetes.

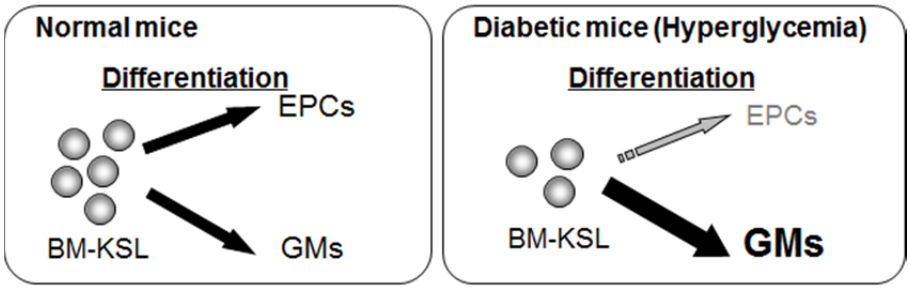

Figure 17　Schematic of regulation mechanism in differentiation from BM-KSL into EPCs and GMs.

4. Conclusions

In this study, the following have been elucidated.

1. EPC colony-forming assay (EPC-CFA), a novel method for assessing the colony-forming potential of EPCs at different differentiation levels, was established in murine EPCs.

2. PB-MNCs, BM-MNCs or BM-KSL differentiated into two types of EPC-CFUs, large-EPC-CFUs and small-EPC-CFUs, which were defined according to cell morphology as spindle-shaped cells or round cells, respectively.

3. Both large- and small-EPC-CFU-derived cells expressed eNOS, Flk-1 and VE-cadherin, markers of ECs.

4. The large-EPCs derived from large-EPC-CFU had higher adhesive capacity but lower proliferative potency than small-EPCs and showed improved tubular forming capacity and incorporation potency into primary EC-derived tube formation.

5. The small-EPCs derived from small-EPC-CFU were higher in number, contained higher population of KSL cells and could differentiate into spindle-shaped cells, large-EPCs, suggesting that small-EPCs might be more immature EPCs.

6. Hindlimb ischemia increased the frequencies of large-EPC-CFUs differentiated from PB-MNCs and BM.

7. Transplantation of large-EPC-CFUs into hindlimb ischemia model enhanced neovascularization, suggesting that large-EPC-CFUs were more functional EPC status for vascular regeneration *in vivo*.

8. T2D mice had fewer BM stem/progenitor cells, a source of EPCs, by regulating the proliferation cascade in *db/db* mice.

9. In T2D mice, the frequency of large-EPC-CFUs derived from BM-KSL was reduced, indicating dysfunction of differentiation into mature EPCs.

10. The BM-KSL of *db/db* mice contained only a small number of CD34(+) cells, which produced more EPC-CFUs than CD34(-) cells, suggesting that the reduced CD34(+) BM-KSL in *db/db* mice may be contributing to their lower frequencies of total EPC-CFUs and large-EPC-CFUs.

11. The BM-KSL of *db/db* mice exhibited a greater potential to differentiate into GMs in spite of the lower differentiation potential into EPCs, suggesting opposing regulatory mechanisms for differentiation into mature EPCs and GMs in T2D mice.

The established murine EPC-CFA highlighted the actual status of EPCs via a redefinition of the differential stages of EPCs through BM-derived stem cells. The understanding of molecular cascades of EPC development from primitive small-EPC-CFUs to definitive large-EPC-CFUs will provide us some useful therapeutic advantages to solve the quantitative or qualitative problems for EPCs therapy.

Using this new EPC-CFA, it was demonstrated that T2D inhibits differentiation into EPCs while promoting differentiation into GMs, suggesting opposing mechanisms in the regulation of differentiation into vascular cells and haematopoietic cells in mice with T2D. Elucidation of the mechanisms underlying these impairments could be helpful in the further development of therapies that work through recovery of BM or EPCs in microvascular and other ischemic diseases in such patients.

Acknowledgements

I would like to express my sincere thanks to Professor Norio Matsuki and Professor Yuji Ikegaya of The University of Tokyo for giving me the opportunity to present this research and their valuable advice.

I would like to greatly appreciate Professor Takayuki Asahara and Associate professor Haruchika Masuda of Tokai University School of Medicine, who gave me appropriate support and advice for carrying out this research.

I am grateful to Dr. Sang-Mo Kwon of Pusan National University for helpful advice on experimental design, support, and discussions.

I thank all my colleagues for helpful discussions and encouragement.

Finally, I am sincerely grateful to my husband, children and parents for their continuous support and encouragement.

References

1. Asahara T, Murohara T, Sullivan A, Silver M, van der Zee R, Li T, Witzenbichler B, Schatteman G, Isner JM. Isolation of putative progenitor endothelial cells for angiogenesis. Science. 1997;275:964–967.
2. Asahara T, Masuda H, Takahashi T, Kalka C, Pastore C, Silver M, Kearne M, Magner M, Isner JM. Bone marrow origin of endothelial progenitor cells responsible for postnatal vasculogenesis in physiological and pathological neovascularization. Circ Res. 1999;85:221–228.
3. Naiyer AJ, Jo DY, Ahn J, Mohle R, Peichev M, Lam G, Silverstein RL, Moore MA, Rafii S. Stromal derived factor-1-induced chemokinesis of cord blood CD34(+) cells (long-term culture-initiating cells) through endothelial cells is mediated by E-selectin. Blood. 1999;94:4011–4019.
4. Isner JM, Asahara T. Angiogenesis and vasculogenesis as therapeutic strategies for postnatal neovascularization. J Clin Invest. 1999;103:1231–1236.
5. Rafii S, Lyden D. Therapeutic stem and progenitor cell transplantation for organ vascularization and regeneration. Nat Med. 2003;9:702–712.
6. Gunsilius E, Petzer AL, Duba HC, Kahler CM, Gastl G. Circulating endothelial cells after transplantation. Lancet. 2001;357:1449–1450.
7. Cho HJ, Kim HS, Lee MM, Kim DH, Yang HJ, Hur J, Hwang KK, Oh S, Choi YJ, Chae IH, Oh BH, Choi YS, Walsh K, Park YB. Mobilized endothelial progenitor cells by granulocyte-macrophage colony-stimulating factor accelerate reendothelialization and reduce vascular inflammation after intravascular radiation. Circulation. 2003;108:2918–2925.
8. Murohara T, Ikeda H, Duan J, Shintani S, Sasaki K, Eguchi H, Onitsuka I, Matsui K, Imaizumi T. Transplanted cord blood-derived endothelial precursor cells augment postnatal neovascularization. J Clin Invest. 2000;105:1527–1536.
9. Kalka C, Masuda H, Takahashi T, Kalka-Moll WM, Silver M, Kearney M, Li T, Isner JM, Asahara T. Transplantation of ex vivo expanded endothelial progenitor cells for therapeutic neovascularization. Proc Natl Acad Sci USA. 2000;97:3422–3427.
10. Kawamoto A, Tkebuchava T, Yamaguchi J, Nishimura H, Yoon YS, Milliken C, Uchida S, Masuo O, Iwaguro H, Ma H, Hanley A, Silver M, Kearney M, Losordo DW, Isner JM, Asahara T. Intramyocardial transplantation of autologous endothelial progenitor cells for therapeutic neovascularization of myocardial ischemia. Circulation. 2003;107:461–468.
11. Kawamoto A, Gwon HC, Iwaguro H, Yamaguchi JI, Uchida S, Masuda H, Silver M, Ma H, Kearney M, Isner JM, Asahara T. Therapeutic potential of ex vivo expanded endothelial progenitor cells for myocardial ischemia. Circulation. 2001;103:634–637.

12. Loomans CJ, de Koning EJ, Staal FJ, Rookmaaker MB, Verseyden C, de Boer HC, Verhaar MC, Braam B, Rabelink TJ, van Zonneveld AJ. Endothelial progenitor cell dysfunction: a novel concept in the pathogenesis of vascular complications of type 1 diabetes. Diabetes. 2004;53:195–199.
13. Tepper OM, Galiano RD, Capla JM, Kalka C, Gagne PJ, Jacobowitz GR, Levine JP, Gurtner GC. Human endothelial progenitor cells from type II diabetics exhibit impaired proliferation, adhesion, and incorporation into vascular structures. Circulation. 2002;106:2781–2786.
14. Hill JM, Zalos G, Halcox JP, Schenke WH, Waclawiw MA, Quyyumi AA, Finkel T. Circulating endothelial progenitor cells, vascular function, and cardiovascular risk. N Engl J Med. 2003;348:593–600.
15. Vasa M, Fichtlscherer S, Aicher A, Adler K, Urbich C, Martin H, Zeiher AM, Dimmeler S. Number and migratory activity of circulating endothelial progenitor cells inversely correlate with risk factors for coronary artery disease. Circ Res. 2001;89:E1–7.
16. Asahara T, Kawamoto A. Endothelial progenitor cells for postnatal vasculogenesis. Am J Physiol Cell Physiol. 2004;287:C572–579.
17. Lin Y, Weisdorf DJ, Solovey A, Hebbel RP. Origins of circulating endothelial cells and endothelial outgrowth from blood. J Clin Invest. 2000;105:71–77.
18. Ingram DA, Mead LE, Tanaka H, Meade V, Fenoglio A, Mortell K, Pollok K, Ferkowicz MJ, Gilley D, Yoder MC. Identification of a novel hierarchy of endothelial progenitor cells using human peripheral and umbilical cord blood. Blood. 2004;104:2752–2760.
19. Yoder MC, Mead LE, Prater D, Krier TR, Mroueh KN, Li F, Krasich R, Temm CJ, Prchal JT, Ingram DA. Redefining endothelial progenitor cells via clonal analysis and hematopoietic stem/progenitor cell principals. Blood. 2007;109:1801–1809.
20. Hur J, Yoon CH, Kim HS, Choi JH, Kang HJ, Hwang KK, Oh BH, Lee MM, Park YB. Characterization of two types of endothelial progenitor cells and their different contributions to neovasculogenesis. Arterioscler Thromb Vasc Biol. 2004;24:288–293.
21. Rohde E, Bartmann C, Schallmoser K, Reinisch A, Lanzer G, Linkesch W, Guelly C, Strunk D. Immune cells mimic the morphology of endothelial progenitor colonies *in vitro*. Stem Cells. 2007;25:1746–1752.
22. Masuda H, Alev C, Akimaru H, Ito R, Shizuno T, Kobori M, Horii M, Ishihara T, Isobe K, Isozaki M, Itoh J, Itoh Y, Okada Y, McIntyre BA, Kato S, Asahara T. Methodological development of a clonogenic assay to determine endothelial progenitor cell potential. Circ Res. 2011;109:20-37.
23. Kwon SM, Eguchi M, Wada M, Iwami Y, Hozumi K, Iwaguro H, Masuda H, Kawamoto A, Asahara T. Specific Jagged-1 signal from bone marrow microenvironment is required for endothelial progenitor cell development for neovascularization. Circulation.

2008;118:157-165.

24. Tanaka R, Wada M, Kwon SM, Masuda H, Carr J, Ito R, Miyasaka M, Warren SM, Asahara T, Tepper OM. The effects of flap ischemia on normal and diabetic progenitor cell function. Plast Reconstr Surg. 2008;121:1929-1942.
25. Kamei N, Kwon SM, Alev C, Ishikawa M, Yokoyama A, Nakanishi K, Yamada K, Horii M, Nishimura H, Takaki S, Kawamoto A, Ii M, Akimaru H, Tanaka N, Nishikawa S, Ochi M, Asahara T. Lnk deletion reinforces the function of bone marrow progenitors in promoting neovascularization and astrogliosis following spinal cord injury. Stem Cells. 2010;28:365-375.
26. Penn MS, Topol EJ. Tissue factor, the emerging link between inflammation, thrombosis, and vascular remodeling. Circ Res. 2001;89:1-2.
27. Surdacki A, Stochmal E, Szurkowska M, Bode-Böger SM, Martens-Lobenhoffer J, Stochmal A, Klecha A, Kawecka-Jaszcz K, Dubiel JS, Huszno B, Szybiński Z. Nontraditional atherosclerotic risk factors and extent of coronary atherosclerosis in patients with combined impaired fasting glucose and impaired glucose tolerance. Metabolism. 2007;56:77-86.
28. Sheetz MJ, King GL. Molecular understanding of hyperglycemia's adverse effects for diabetic complications. JAMA. 2002;288:2579-2588.
29. Saad MI, Abdelkhalek TM, Saleh MM, Kamel MA, Youssef M, Tawfik SH, Dominguez H. Insights into the molecular mechanisms of diabetes-induced endothelial dysfunction: focus on oxidative stress and endothelial progenitor cells. Endocrine. 2015;50:537-567.
30. Drake CJ, Fleming PA. Vasculogenesis in the day 6.5 to 9.5 mouse embryo. Blood. 2000;95:1671–1679.
31. Takahashi T, Kalka C, Masuda H, Chen D, Silver M, Kearney M, Magner M, Isner JM, Asahara T. Ischemia- and cytokine-induced mobilization of bone marrow-derived endothelial progenitor cells for neovascularization. Nat Med. 1999;5:434–438.
32. Ceradini DJ, Kulkarni AR, Callaghan MJ, Tepper OM, Bastidas N, Kleinman ME, Capla JM, Galiano RD, Levine JP, Gurtner GC. Progenitor cell trafficking is regulated by hypoxic gradients through HIF-1 induction of SDF-1. Nat Med. 2004;10:858–864.
33. Fadini GP, Sartore S, Schiavon M, Albiero M, Baesso I, Cabrelle A, Agostini C, Avogaro A. Diabetes impairs progenitor cell mobilisation after hindlimb ischaemia-reperfusion injury in rats. Diabetologia. 2006;49:3075–3084.
34. De Falco E, Porcelli D, Torella AR, Straino S, Iachininoto MG, Orlandi A, Truffa S, Biglioli P, Napolitano M, Capogrossi MC, Pesce M. SDF-1 involvement in endothelial phenotype and ischemia-induced recruitment of bone marrow progenitor cells. Blood. 2004;104:3472–3482.
35. Li SL, Reddy MA, Cai Q, Meng L, Yuan H, Lanting L, Natarajan R. Enhanced proatherogenic responses in macrophages and vascular smooth muscle cells derived from diabetic *db/db* mice. Diabetes. 2006;55:2611-2619.

36. O'Connor JC, Satpathy A, Hartman ME, Horvath EM, Kelley KW, Dantzer R, Johnson RW, Freund GG. IL-1beta-mediated innate immunity is amplified in the *db/db* mouse model of type 2 diabetes. J Immunol. 2005;174:4991-4997.
37. Zykova SN, Jenssen TG, Berdal M, Olsen R, Myklebust R, Seljelid R. Altered cytokine and nitric oxide secretion *in vitro* by macrophages from diabetic type II-like *db/db* mice. Diabetes. 2000;49:1451-1458.
38. Fadini GP, Sartore S, Albiero M, Baesso I, Murphy E, Menegolo M, Grego F, Vigili de Kreutzenberg S, Tiengo A, Agostini C, Avogaro A. Number and function of endothelial progenitor cells as a marker of severity for diabetic vasculopathy. Arterioscler Thromb Vasc Biol. 2006;26:2140-2146.
39. Tamarat R, Silvestre JS, Le Ricousse-Roussanne S, Barateau V, Lecomte-Raclet L, Clergue M, Duriez M, Tobelem G, Lévy BI. Impairment in ischemia-induced neovascularization in diabetes: bone marrow mononuclear cell dysfunction and therapeutic potential of placenta growth factor treatment. Am J Pathol. 2004;164:457-466.
40. Asahara T, Takahashi T, Masuda H, Kalka C, Chen D, Iwaguro H, Inai Y, Silver M, Isner JM. VEGF contributes to postnatal neovascularization by mobilizing bone marrow-derived endothelial progenitor cells. EMBO J. 1999;18:3964-3972.
41. Yamaguchi J, Kusano KF, Masuo O, Kawamoto A, Silver M, Murasawa S, Bosch-Marce M, Masuda H, Losordo DW, Isner JM, Asahara T. Stromal cell-derived factor-1 effects on ex vivo expanded endothelial progenitor cell recruitment for ischemic neovascularization. Circulation. 2003;107:1322-1328.
42. Segal MS, Shah R, Afzal A, Perrault CM, Chang K, Schuler A, Beem E, Shaw LC, Li Calzi S, Harrison JK, Tran-Son-Tay R, Grant MB. Nitric oxide cytoskeletal-induced alterations reverse the endothelial progenitor cell migratory defect associated with diabetes. Diabetes. 2006;55:102-109.
43. Nikolic T, Bunk M, Drexhage HA, Leenen PJ. Bone marrow precursors of nonobese diabetic mice develop into defective macrophage-like dendritic cells *in vitro.* J Immunol. 2004;173:4342-4351.
44. Chilton PM, Rezzoug F, Ratajczak MZ, Fugier-Vivier I, Ratajczak J, Kucia M, Huang Y, Tanner MK, Ildstad ST. Hematopoietic stem cells from NOD mice exhibit autonomous behavior and a competitive advantage in allogeneic recipients. Blood. 2005;105:2189-2197.
45. Hotamisligil GS. Inflammation and metabolic disorders. Nature. 2006;444:860-867.
46. Shoelson SE, Lee J, Goldfine AB. Inflammation and insulin resistance. J Clin Invest. 2006;116:1793-1801.
47. Wellen KE, Hotamisligil GS. Inflammation, stress, and diabetes. J Clin Invest. 2005;115:1111-1119.

48. Dandona P, Aljada A, Bandyopadhyay A. Inflammation: the link between insulin resistance, obesity and diabetes. Trends Immunol. 2004;25:4-7.
49. Halaas JL, Gajiwala KS, Maffei M, Cohen SL, Chait BT, Rabinowitz D, Lallone RL, Burley SK, Friedman JM. Weight-reducing effects of the plasma protein encoded by the obese gene Science. 1995;269:543-546.
50. Lee GH, Proenca R, Montez JM, Carroll KM, Darvishzadeh JG, Lee JI, Friedman JM. Abnormal splicing of the leptin receptor in diabetic mice. Nature. 1996;379:632-635.
51. Hayase M, Ogawa Y, Katsuura G, Shintaku H, Hosoda K, Nakao K. Regulation of obese gene expression in KK mice and congenic lethal yellow obese *KKAy* mice. Am J Physiol. 1996;271:E333-E339.
52. Hounsom L, Tomlinson DR. Does neuropathy develop in animal models? Clin Neurosci. 1997;4:380-389.
53. Stepanovic V, Awad O, Jiao C, Dunnwald M, Schatteman GC. Leprdb diabetic mouse bone marrow cells inhibit skin wound vascularization but promote wound healing. Circ Res. 2003;92:1247-1253.
54. Awad O, Jiao C, Ma N, Dunnwald M, Schatteman GC. Obese diabetic mouse environment differentially affects primitive and monocytic endothelial cell progenitors. Stem Cells. 2005;23:575-583.